REVIEW ARTICLE

Experimental review on Hypernuclear Physics: recent achievements and future perspectives

A Feliciello[1] and T Nagae[2]

[1] Istituto Nazionale di Fisica Nucleare - Sezione di Torino
Via P. Giuria 1, I-10125 Torino, Italy

E-mail: `Alessandro.Feliciello@to.infn.it`

[2] Kyoto University, Department of Physics
Kitashirakawa, Sakyo-ku, Kyoto 606-8502, Japan

E-mail: `nagae@scphys.kyoto-u.ac.jp`

Abstract.
After the shutdown of several old proton synchrotons, which played a fundamental role for the second generation experiments of hypernuclear physics performed in Europe, USA and Japan, some new experimental setups aiming to achieve sub-MeV energy resolution have been operated for a long time. In the last decade the hypernuclear physics community was committed to carrying on several third generation experiments, by exploiting the potentialities offered by new accelerators, such as a continuous electron beam machine and a ϕ-factory. Large data samples were collected on specific items, thanks to dedicated facilities and experimental apparatuses. The attention was mainly focused on both high-resolution spectroscopy and decay mode study of single Λ-hypernuclei. Nowadays this phase is over but, until recently, important and to some extent unexpected results were achieved. Un updated review of selected experimental results is presented as well as a survey of the perspectives for future studies.

30 April 2015

Contents

1. Introduction

Hypernuclear physics, also known as strangeness nuclear physics, is a branch of nuclear physics devoted to the study of bound nuclear systems where one (or more) constituent nucleons is (are) replaced by one (or more) hyperons (Λ, Σ, Ξ, Ω), that is baryons with strangeness quantum number $S \neq 0$. Such investigations have a large impact on present-day physics: actually they lie at the intersection of nuclear and elementary particle physics and they have, in addition, important implications for astrophysics.

In the second half of the 20th century, investigations of hypernuclei evolved in various aspects. The definition of a hypernuclear object was extended from Λ-hypernuclei to Σ-, double Λ- and Ξ-hypernuclei. There was a great progress in production methods by using both K^- and π^+ beams. A lot of modern experimental techniques were adopted for hypernuclear spectroscopy. Not only the production of hypernuclei but also their structure and their decay properties were addressed as research subjects.

In the beginning of the 21st century, electron beams were introduced for the first time as a tool to produce Λ-hypernuclei. The (K^-_{stop}, π^-) reaction has been revisited by using a monochromatic low-energy K^- source. In these studies, the energy resolution of magnetic spectrometers has been improved from a few MeV to the sub-MeV level. Many new results have been brought to the scientific community. Fortunately, there are still new facilities to carrying on promising experimental programs such as the Japan Proton Accelerator Research Complex (J-PARC). An electron beam facility is now in operation at Mainz and a next generation one is planned at Jefferson Lab (JLab). A new facility for antiprotons and ions (FAIR) is now under construction. Then, it is a good time to review the experimental achievements in last ten years and give future perspectives for the coming decade.

The most up-to-date topics in this research field can be found in the proceedings of a series of International Conferences on Hypernuclear and Strange Particle Physics (HYP Conference). The last three conferences were held in Barcelona (HYP-XI, 2012) [1], in Tokai, J-PARC (HYP-X, 2009) [2] and in Mainz (HYP2006, 2006) [3].

Early works in the beginning of Hypernuclear Physics were well summarized in two papers [4, 5] by two pioneers in this field, when the fifty years of hypernuclear physics were celebrated during the HYP2003 conference at Newport News [6]. Both experimental and theoretical progress achieved in the decade from 1970 to 1980 can be found in several review articles [7–9]. The status of the newly developed hypernuclear spectroscopy with the (π^+, K^+) and (e, $e'K^+$) reactions and hypernuclear γ-ray measurements in the 1990s and the 2000s were reviewed in 2006 by Hashimoto and Tamura [10]. The recent review article published in 2012 by Botta, Bressani and Garbarino [11] covers not only the further progress in hypernuclear spectroscopy but also new subjects of neutron-rich Λ-hypernuclei, anti-kaonic nuclear clusters and advances in weak decay studies. Several lecture notes of international schools [12–14] are also available for graduate students.

The scope of the present article is intended to review experimental progress mainly after the HYP2003 conference. The paper is organized as follows. In Section 2 basic experimental observables and measurement methods are introduced; moreover the physics interests from these outputs are discussed. In Section 3 we will provide a brief historical overview of this research field and the roles of major facilities which supported these experimental advancements. Section 4 summarizes the recent progress in hypernuclear spectroscopy of single Λ-hypernuclei. In particular, production of

neutron-rich Λ-hypernuclei is discussed. Section 5 covers the advancements in both mesonic and non-mesonic weak decay studies. In Section 6, studies of other hypernuclei such as Σ-, Ξ- and double Λ-hypernuclei are reviewed. The new research field of anti-hypernuclei produced in high-energy heavy-ion collisions is briefly discussed in Section 7. Another new research field recently came on the scene is the investigation on deeply-bound $\overline{K}$-nuclei, which is reviewed in Section 8. Finally, in Section 9, the future perspectives offered by several experimental facilities in the world, both in operation and in preparation, are described.

2. Hypernuclear Physics in a nutshell

2.1. Physics motivations, observables, general definitions

Interest in studying hypernuclei is manyfold. It ranges from the curiosity to observe the behavior of such many-body nuclear systems to the desire to discover possible implications on the theory of strong nuclear forces in the non-perturbative regime. The conventional notation for a hypernucleus is $^A_Y Z$, where the mass number $A = N+Z+Y$ stands for the total number of baryons in the system (including neutrons, protons and hyperons), Y is the symbol of embedded hyperon(s) and Z indicates the electric charge. In the case of charge-neutral hyperon, the Z corresponds to the number of protons, i.e. to the nuclear species, while for negative-charge hyperon, like Σ^- and Ξ^-, care should be taken.

Investigations of hypernuclei deal with three aspects: production, structure and decay. As for the production of $S = -1$ hypernuclei, two types of reactions are usually exploited: $p_1(S = 0) + A(S = 0) \rightarrow p_2(S = +1) + B(S = -1)$ or $p_1(S = -1) + A(S = 0) \rightarrow p_2(S = 0) + B(S = -1)$. Here, $A(S = 0)$ is the experimental target and $B(S = -1)$ is the produced hypernucleus. Since they are simple two-body reactions, by measuring the four-momenta of particles p_1 and p_2, it is possible to measure the mass of a hypernucleus B as a missing-mass expressed as

$$M_B = \sqrt{\{E_{p_2} - (M_A + E_{p_1})\}^2 - \{\vec{p}_{p_2} - \vec{p}_{p_1}\}^2}, \qquad (2.1)$$

where E_{p_i} and $\vec{p}_{p_i}$ are the energy and the three-momentum vector of particle i and M_A is the mass of target nucleus A. Then, the binding energy of the hypernucleus is obtained as

$$-B = M_B - (M_{A-1} + M_{\Lambda/\Sigma}), \qquad (2.2)$$

where M_{A-1} is the mass of the core nucleus composed of $A-1$ nucleons and $M_{\Lambda/\Sigma}$ is the mass of the hyperon. When the ground state binding energy is determined, then excitation energies of those states are obtained as the binding energy differences.

In the (K^-, π^-) and (π^+, K^+) reactions, it is necessary to measure the four momenta of kaons and pions, so that two spectrometers are needed. In the $(K^-_{\text{stop}}, \pi^-)$ reaction, $\vec{p}_{p_1} = 0$ and $E_{p_1} = M_{K^-}$, then just one spectrometer to measure pions is enough. The production of $S = -2$ bound states, Ξ- and double Λ-hypernuclei, can be achieved in the same way via the $\Delta S = +2$ (K^-, K^+) reaction with a two spectrometer system.

The other way to measure the binding energy is to use a kind of invariant-mass method. Light Λ-hypernuclei weakly decay from the ground state to $B \rightarrow \pi^-(+p)+C$ in sizeable fractions of the order of 10%. By detecting all the charged particles in the final state, $\pi^-(+p)+C$, it is possible to reconstruct the mass of the parent hypernucleus

B without knowing how it is produced. This is the usual case in the nuclear emulsion technique owing to its superb space resolution of ~ 1 μm. There is a special case in which the final state is in two-body kinematics as $\pi^- + C$. When the decay occurs after the stopping of B, the π^- energy uniquely gives the mass of B as a mono-energetic peak.

The produced hypernuclear levels strongly depend on the production mechanism, which will be discussed in subsection 2.4. Therefore, the structure information obtained is also reaction-dependent. Some important parameters involved are momentum transfer between p_1 and p_2, spin-flip strength, charge exchange, etc..

As will be discussed in Section 5, Λ-hypernuclei decay through weak processes. While the lifetime of Λ in free space is $(2.631 \pm 0.020) \times 10^{-10}$ s, the lifetime (τ) of Λ-hypernuclei is a bit shorter but always of the order of ~ 200 ps. The main decay mode for light Λ-hypernuclei is mesonic weak decay emitting a pion (π^-, π^0). In medium to heavy systems, non-mesonic weak decay processes $(\Lambda \mathcal{N} \to \mathcal{N} \mathcal{N}, \Lambda \mathcal{N} \mathcal{N} \to \mathcal{N} \mathcal{N} \mathcal{N})$ become dominant because of the Pauli blocking to the mesonic weak decay processes. Thus, for each decay process, the decay rate obeys the following relation,

$$\Gamma_{\text{total}} = \frac{1}{\tau} = \Gamma_{\text{MWD}} + \Gamma_{\text{NMWD}}, \qquad (2.3)$$

where Γ_{MWD} and Γ_{NMWD} are the decay rates for the mesonic and the non-mesonic weak decay modes. The mesonic mode is split into $\Gamma_{\text{MWD}} = \Gamma_{\pi^-} + \Gamma_{\pi^0}$ with two different pion charge modes. As for the non-mesonic modes, the $\Gamma_{\text{NMWD}} = \Gamma_{\Lambda \mathcal{N} \to \mathcal{N} \mathcal{N}} + \Gamma_{\Lambda \mathcal{N} \mathcal{N} \to \mathcal{N} \mathcal{N} \mathcal{N}} \equiv \Gamma_{1\mathcal{N}} + \Gamma_{2\mathcal{N}}$ with one-nucleon induced and two-nucleon induced modes. The one-nucleon induced mode is categorized with two modes as $\Gamma_{1\mathcal{N}} = \Gamma_n + \Gamma_p$. Since the non-mesonic mode is peculiar in Λ-hypernuclei, the reaction mechanism has been intensively investigated both theoretically and experimentally. Recent experimental progress allows us to investigate the Γ_n branch by directly measuring the two neutrons in coincidence and to access the $\Gamma_{2\mathcal{N}}$ by detecting very low-energy nucleons.

The reaction mechanism of the mesonic weak decay is rather well understood phenomenologically. By using this property, the ground state spin and parity has been determined for several light Λ-hypernuclei such as $^3_\Lambda$H$(1/2^+)$, $^4_\Lambda$H(0^+), $^4_\Lambda$He(0^+), $^8_\Lambda$Li(1^-), etc. by measuring the pion decay angular distribution and so on [4].

2.2. Baryon-baryon interaction in SU(3)

The so-called realistic nuclear force model has been constructed based on a lot of systematic low-energy $p - p$ and $p - n$ scattering data from about 4300 experimental points, including various polarization data. Thus, we have good descriptions of nuclei based on this $\mathcal{N} \mathcal{N}$ interaction model. On the contrary, knowledge of hyperon-proton $(Y - p)$ scattering is very limited due to the small data sample available, consisting of 38 experimental points only. This is because low energy hyperon beams decay in a few cm ($c\tau = 7.89$, 2.40, 4.43, 4.91 cm for Λ, Σ^+, Σ^-, Ξ^-, respectively) so that it is hard to observe scattering events before the decay, even when an active target, which works as a production target of hyperon and as a scattering target at the same time, is used. Very high-intensity hyperon beams are required in order to accumulate statistics comparable with those available for $\mathcal{N} - \mathcal{N}$ scattering. Of course, a hyperon target cannot be prepared, so that $Y - Y$ scattering measurements are impossible.

An extension of our knowledge on the $\mathcal{N} \mathcal{N}$ interaction to flavor $SU(3)$, $Y \mathcal{N}$ and YY interactions, is not trivial. In $SU(3)_F$, baryon octet to octet $(8 \otimes 8)$ interactions

are categorized as $27_s \oplus 8_s \oplus 1_s \oplus 10_a^* \oplus 10_a \oplus 8_a$. The $\mathcal{N}\mathcal{N}$ interaction just gives us information on 27_s and 10_a^* only. Note that the famous H dibaryon [15] belongs to 1_s. Therefore, a lack of $Y\mathcal{N}$ and YY scattering data has been a handicap to fully understand the baryon-baryon interaction in $SU(3)_F$.

In this respect, it is still effective to obtain information on $Y\mathcal{N}$ and YY interactions from the spectroscopic studies of hypernuclei. Double Λ-hypernuclei give us very unique information on the $\Lambda - \Lambda$ interaction. In particular, in the case of p-shell Λ-hypernuclei, the fine level structures of hypernuclei observed in hypernuclear γ-ray spectroscopy [16] were well described with an effective $\Lambda\mathcal{N}$ interaction [17] expressed as

$$V_{\Lambda\mathcal{N}}^{eff}(r) = V_0(r) + V_\sigma(r)\vec{s}_\Lambda \cdot \vec{s}_\mathcal{N}$$
$$+ V_\Lambda(r)l_{\Lambda\mathcal{N}} \cdot \vec{s}_\Lambda + V_\mathcal{N}(r)l_{\Lambda\mathcal{N}} \cdot \vec{s}_\mathcal{N} + V_T(r)S_{12} \qquad (2.4)$$

where $S_{12} = 3(\vec{\sigma}_\Lambda\hat{r})(\vec{\sigma}_\mathcal{N}\hat{r}) - \vec{\sigma}_\Lambda\vec{\sigma}_\mathcal{N}$ is the tensor operator, $\vec{r} = \vec{r}_\mathcal{N} - \vec{r}_\Lambda$ is the relative $\Lambda\mathcal{N}$ coordinate, $\vec{s}_\mathcal{N}$ ($\vec{s}_\Lambda$) is the nucleon (hyperon) spin operator and $l_{\Lambda\mathcal{N}}$ is the $\Lambda\mathcal{N}$ relative angular momentum operator. From the γ-ray data, it is possible to estimate the strength of the $\Lambda\mathcal{N}$ spin-spin interaction V_σ, of the spin-orbit interactions V_Λ and $V_\mathcal{N}$ and of the tensor force V_T. The potential well depth in nuclear matter is well constrained by the mass-number dependence of the ground-state binding energies in heavy Λ-hypernuclei. It depends on both V_0 and the strength of the three-body $\Lambda\mathcal{N}\mathcal{N}$ interaction. In addition, a measurable effect of the $\Lambda - \Sigma$ coupling is to provide not negligible contributions to level spacings in the p-shell Λ-hypernuclei.

There exist various baryon-baryon interaction models in different theoretical approaches. Here, a list of the ones usually used for hypernuclear physics is reported. The Nijmegen models are intensively applied for hypernuclear calculations based on one-boson exchange and, recently, on extended soft-core model [18–20]. They try to reproduce the latest hypernuclear spectroscopic data such as $V_0^\Lambda \approx$ -28 MeV, $V_\Sigma \approx +30$ MeV, and $V_\Xi \approx$ -14 MeV and small Λ spin-orbit force. The Jülich Group developed two types of models: one is based on Effective Field Theory extended to the flavor $SU(3)$ [21, 22]; the other is based on meson exchange [23]. Quark-cluster models are also frequently used [24, 25].

One remarkable example of recent progress in baryon-baryon interaction model building is that the baryon-baryon potential can be obtained with lattice QCD technique [26]. The technique was naturally applied to strangeness sector [27–29]. Although they still need to use some approximations to speed up algorithms, realistic calculations should soon be available.

2.3. Role of strangeness in high-density nuclear matter

In ordinary nuclei, the central nucleon density saturates at $\rho_0 \approx 0.16$ fm^{-3}. Therefore, the information of short-range part (< 0.5 fm) of nuclear force is not essential to describe the typical nuclear properties.

On the other hand, when one deals with high-density nuclear matter characterized by a density higher than 2-4 ρ_0, a treatment of the repulsive core becomes essential and short-range behavior becomes important. In this region, the present realistic nuclear force models have large uncertainties. At the same time, the nucleon Fermi energy becomes high enough to produce hyperons: $\Lambda(1116)$, $\Sigma^-(1197)$, $\Sigma^0(1193)$ and so on. Typically, at a nuclear matter density $\sim$2-3 ρ_0 the lightest hyperon Λ is supposed

to appear. This density threshold value depends on the Λ potential in such a high-density nuclear matter. Therefore, it is important to understand the hyperon potential in nuclear matter through hypernuclear binding energy measurements at large mass number A.

There is another important argument related to charge conservation. In high-density nuclear matter, the electron Fermi energy is so high because of the small electron mass. Therefore, negatively-charged hyperons such as Σ^- and Ξ^- tend to easily be produced by absorbing the electron energy. Note that the existence of negatively charged baryons is unique in strangeness sector. Measurements of the potential depths of these particles are important in this respect. In fact, if the Σ^- potential was strongly attractive, Σ^- could appear at a density value even lower than the one for the Λ.

Because of the saturation property of the nuclear central density, the investigation of high-density nuclear matter is not easily realized experimentally. For high temperature environments, heavy ion collisions at energy ≥ 200 A GeV are a good tool, which is established both at the BNL Relativistic Heavy Ion Collider (RHIC) and the CERN Large Hadron Collider (LHC). However, what kind of baryon density is realized in heavy ion collisions at around 20 A GeV, in which the highest baryon density is expected to be reached, is still an open question. Looking into the Universe, it is theoretically expected that such a high-density nuclear matter environment is realized inside a neutron star. Typical neutron star mass is 1-2 times the solar mass ($M_\odot$) and the radius is 10–12 km. The density at the core of neutron star might be in the range of 4-8 ρ_0. Therefore, strangeness degree of freedom should have a significant role in neutron star.

The presence of strangeness in neutron star could influence several aspects. The most important one is the mass-radius relation obtained from the equation of state (EoS) of such high-density nuclear matter. In the case of pure nucleonic high-density matter, the prediction for the maximum neutron star mass ranges from 1.8 to 2.4 $M_\odot$. However, the introduction of hyperons softens the EoS and the maximum mass is reduced to be less than 1.5 $M_\odot$ with a compact size. It is actually possible to reduce the degeneracy pressure of the neutron matter by introducing hyperon degrees of freedom. However, the recent observation of ~ 2 $M_\odot$ neutron stars, PSR J1614-2230 (1.97 ± 0.04 $M_\odot$) [30] and PSR J0348-0432 (2.01 ± 0.04 $M_\odot$) [31], forces us to confront the so called "hyperon puzzle". It is not easy to support the existence of such large mass objects ($> 2 M_\odot$) containing hyperonic matter. A lot of theoretical ideas are now proposed to somehow resolve the puzzle.

Strangeness plays another role in neutron stars as far as their cooling is concerned. The presence of hyperons provides an additional mechanism that makes the cooling process faster thanks to, for instance, neutrino emission through the $Y \to B + l + \bar{\nu}_l$ reaction. However, hyperon superfluidity tends to suppress the faster cooling. So the quantitative estimation of hyperon pairing has received much attention in these days.

In the new generation of gravitational wave observatories in the world, the gravitational wave emitted during the neutron star-neutron star (NS-NS) merger is supposed to be a good indicator of the source. Numerical simulations of the NS-NS merger are carried out based on the EoS of neutron star. These studies suggest that the gravitational wave pattern could be sensitive to the neutron star EoS. Thus, the detection of gravitational wave from the NS-NS merger is eagerly awaited.

2.4. Hypernucleus production methods

As already mentioned in the Introduction, a hypernucleus is an unstable nucleus where one or more nucleons are replaced by one or more hyperons, usually Λ particles.

Danysz and Pniewski observed the first hypernucleus, or better, the first hyperfragment following the interaction of a high energy cosmic ray in a stack of photographic emulsions [32]. Since then, different methods were exploited at accelerators to produce higher and higher statistics data samples and different species of hypernuclei in a well defined initial state. Such a task is only apparently easy to accomplish and it actually represents one of the main challenges in experimental hypernuclear physics.

Most of the experimental data available today were basically obtained thanks to the following two-body reactions, aiming to implant an explicit strangeness content inside an ordinary nucleus. A hypernucleus can be then regarded as the outcome of a genetic engineering manipulation, applied to the nuclear physics domain.

The most natural and intuitive solution is to irradiate a nuclear target with a beam of strange particles. It is the case of strangeness exchange reactions

$$K^- + n \rightarrow \Lambda + \pi^- \qquad (\bar{u}s + udd \rightarrow uds + \bar{u}d), \qquad (2.5a)$$

$$K^- + p \rightarrow \Lambda + \pi^0 \qquad (\bar{u}s + uud \rightarrow uds + u\bar{u}) \qquad (2.5b)$$

induced by kaons both in flight and at rest. Such processes can be ultimately considered as a transfer of a s-quark from the projectile meson to the target nucleon and they are preferentially studied in the charge state $(2.5a)$, due to the evident advantage in measuring the final state π^- momentum spectrum rather than performing precise spectroscopy using the π^0 from $(2.5b)$.

A more efficient alternative is the so called associated production reaction

$$\pi^+ + n \rightarrow \Lambda + K^+ \qquad (u\bar{d} + udd \rightarrow uds + u\bar{s}) \qquad (2.6)$$

where the incident meson creates a $s\bar{s}$ pair.

The recent improvement of the quality of e^- beams and, moreover, of their duty cycle, offers a further opportunity, by making possible the so called electro-production of hypernuclei at a reasonable rate, despite of the low cross section of the elementary process

$$e^- + p \rightarrow e^{-\prime} + \Lambda + K^+. \qquad (2.7)$$

The virtual photon emitted in such a reaction can be considered quasi-real; then process (2.7) is usually referred to as a two-body photo-production reaction

$$\gamma + p \rightarrow \Lambda + K^+ \qquad (uud \rightarrow uds + u\bar{s}) \qquad (2.8)$$

where this time the $s\bar{s}$ pair is created by the interaction between the incident photon and the target nucleon.

It is worth noting that, neglecting the experimental difficulty associated with the choice, it is possible to select the neutron to proton (N/Z) balance of produced hypernuclei. In processes $(2.5a)$ and (2.6) a neutron of the initial nucleus is replaced by a Λ, while in reactions $(2.5b)$ and (2.7) it is a proton to be transformed in a hyperon; this way it is possible to produce pairs of neutron-rich mirror hypernuclei by using the same target.

Each of the above mentioned processes has its advantages and its drawbacks from both the physical and the technical point of view. In fact, they can be classified in terms of the cross section for the elementary process, the internal quantum number
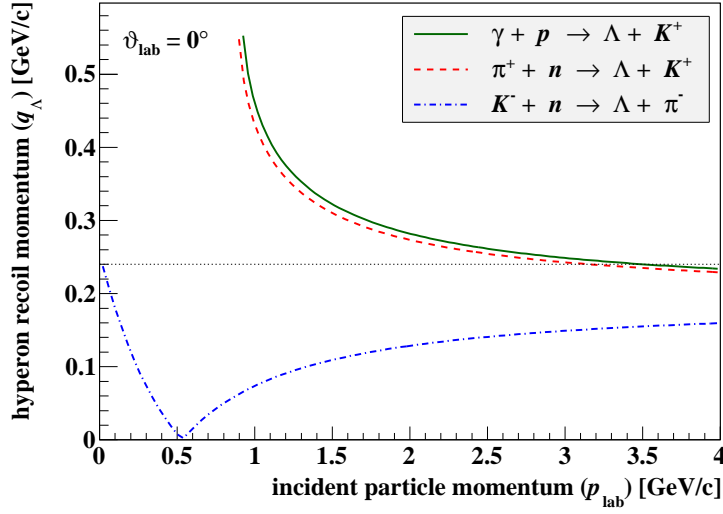
Figure 1. Kinematics of reactions $(2.5a)$, (2.6) and (2.8) for Λ forward emission $(\vartheta_{lab} = 0°)$. The momentum transferred to the hyperon is plotted as a function of the incident particle $(K^-, \pi^+$ or $\gamma)$ momentum in the laboratory frame.

transfer and the modification of the incoming and outgoing particle properties due to the nuclear target absorption. However, the most significant parameter to determine the selectivity and the effectiveness of reactions $(2.5a)$-(2.7) is the momentum transfer to the produced hyperon. Figure 1 shows the trend of the Λ recoil momentum (q_Λ) plotted against the projectile momentum in the laboratory frame (p_{lab}), evaluated for reactions $(2.5a)$, (2.6) and (2.8) when the Λ is forward emitted $(\vartheta_{lab} = 0°)$. A comparison of the different curves shows significant kinematical differences: for process $(2.5a)$, which is exothermic with a Q value of ~ 178 MeV, there exists a value of p_{lab} (505 MeV/c), usually known as "magic momentum" [33], at which q_Λ vanishes and recoilless Λ production takes place; on the contrary, for reaction (2.6), which is endothermic with a Q value of ~ -530 MeV, q_Λ decreases monotonically with p_{lab}, staying always at values exceeding 200 MeV/c. A further tuning of the value of q_Λ can be achieved by a suitable choice of the angular acceptance window for the final state meson. One last, important point to keep in mind is that the value of q_Λ achievable in reaction $(2.5a)$ induced by stopped K^- is comparable with the one typical of processes (2.6) and (2.7).

Another argument that could be taken into account when comparing the different production methods is the possibility of selecting the hypernuclear quantum numbers. By using reaction $(2.5a)$ with K^- in flight, hypernuclear substitutional states are preferentially populated: they are actually obtained by converting a neutron of the original nucleus into a Λ, by keeping it in the same orbit and spin state, without any angular momentum transfer. On the other hand, the large momentum transfer occurring in processes $(2.5a)$ with K^- at rest, (2.6) and (2.7) permits the excitation of high-spin hypernuclear states. This situation offers an ideal playground to perform hypernuclear spectroscopy studies and investigations on weak decay as well. Finally, since both reactions $(2.5a)$ and (2.6) are characterized by small spin-flip amplitudes
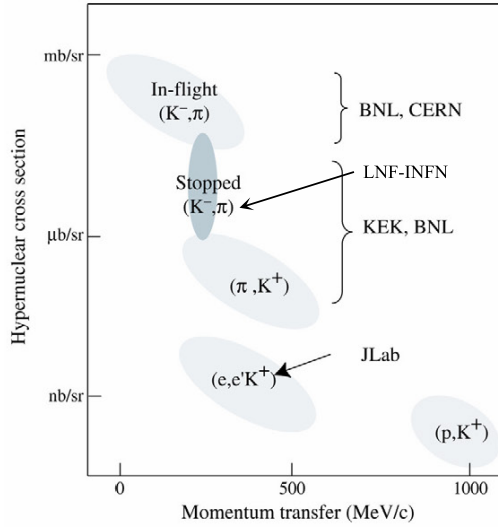
Figure 2. Cross section for typical hypernuclear production reaction as a function of the transferred momentum (adapted from [10]).

they populate mainly non-spin-flip hypernuclear states. On the contrary, process (2.7) amplitude has a sizeable spin-flip component even at $\vartheta_{lab} = 0°$ due to the spin 1 of the photon; then both non-spin-flip and spin-flip hypernuclear states with unnatural parities can be formed in electro-production of hypernuclei.

As far as the reaction cross section is concerned, strangeness exchange processes (2.5a) and (2.5b) are characterized by a relatively large value, of the order of mb/sr; however the intensity and the quality of kaon beams are still today an issue. The cross section value for associate production reaction (2.6) is lower by as many as three orders of magnitude ($\sim \mu$b/sr) but available pion beams permit measurements in a reasonable amount of time. A further three orders of magnitude separates the cross section for the photo-production reaction (2.7) which is of the order of nb/sr and, as already pointed out, only the recent improvement of accelerator performance enabled the exploitation of this process to carry out an experiment. The situation is well summarized by figure 2‡.

Finally, it should be mentioned that hypernuclei were produced also in $\bar{p}$ annihilations [34] or in heavy-ion collisions [35–38].

Recent comparative and critical reviews of the different exploitable hypernucleus production methods can be found in [10, 39, 40].

2.5. Hypernuclear spectroscopy

Since the observation of the first hyperfragment formation event [32], the spectroscopic study of Λ-hypernuclei has been the best experimental method to investigate the hyperon-nucleon ($\Lambda\mathcal{N}$) interaction. It is possible to distinguish between missing-mass (or reaction) spectroscopy and γ-ray spectroscopy, which are to a large

‡ as far as the hypernuclei production via the reaction (2.5a) with K^- at rest is concerned, it should be better to speak in terms of capture rate, instead of cross section.

extent complementary approaches. Missing-mass spectroscopy, based on a precise measurement of the momentum of the companion particle of the Λ-hypernucleus in the two-body formation reactions (2.5a), (2.5b), (2.6) and (2.8), allows an assessment of the gross features of the $\Lambda\mathcal{N}$ force, namely the central, spin-independent, part of the interaction through the determination of hypernuclear masses, of hyperon binding energies and of production reaction cross sections. The main limiting factor of this investigation technique is the momentum resolution achievable on the final state particles. In the long series of experiments performed since the early 70s at CERN, BNL, KEK and LNF with the reactions (2.5a) and (2.6), it was generally not less than 1 MeV [10] and only very recently the process (2.7) studied at JLab made possible to reach a sub-MeV performance [41]. Nevertheless, the observed excitation spectra for a large variety of Λ-hypernuclei, ranging from $^{3}_{\Lambda}$H to $^{208}_{\Lambda}$Pb, were rather well understood in the framework of the distorted wave impulse approximation (DWIA) calculations, based on the shell model [42]. The observed hypernuclear states were instead interpreted with shell-model [43] and cluster-model [44] calculations. With the exception of s- and p-shell Λ-hypernuclei, mean field models based on Wood-Saxon Λ-nucleus potentials satisfactorily reproduced the hypernuclear mass dependence of the hyperon binding energies in the various orbits, determined by the reaction spectroscopy experiments by using a nuclear radius value r = $1.1(A-1)^{1/3}$ fm and a potential depth of 28–30 MeV [45]: actually, the real part of the Λ-nucleus potential turned out to be $\Re(V_{\Lambda}(\rho_0)) \sim -(28$–$30)$ MeV. The fact that such a simple mean field picture provides a fairly accurate description of the overall hypernuclear properties means that the hyperon, being distinguishable particle, maintains its single-particle behavior in the nuclear medium; this is true even for states well below the Fermi surface, a property not observed in the case of nucleons. Finally, since the Pauli blocking is not effective on the Λ, it has the capability of sitting on any single-particle energy level, located in the deeper part of the nucleus core, and then of playing a stabilizing role in the hypernuclear system [46].

γ-ray spectroscopy is an established technique which, thanks to the keV energy resolution achievable using High Purity Germanium (HPGe) detectors, provided deep insights into nuclear structure. The exploitation of the performance of HPGe crystal based devices is even more fundamental for hypernuclear spectroscopy. Owing to the weakness of the hyperon-nucleon interaction, the weak-coupling picture is able to describe in a satisfactory way simple hypernuclear systems, where a Λ in s-shell is coupled to a (ground-state) nuclear core. In such a scheme, the presence of the Λ hyperon causes the splitting of each core nucleus state with non-zero spin (J_c) into a doublet ($J = J_c \pm 1/2$), due to the spin dependent components of the $\Lambda\mathcal{N}$ interaction (spin-spin, spin-orbit and tensor terms of equation (2.4)). The typical energy spacing of such doublets is of the order of 10–100 keV. Then the excellent energy resolution of HPGe detectors is mandatory to resolve the spin doublets in Λ-hypernuclei, by measuring the energy of γ-rays emitted during transitions connecting different doublets or from the upper to the lower member of the same doublet. This way it is possible to determine what is generally referred to as hypernuclear fine structure. Unfortunately, this methodology could not be applied to hypernuclear physics for long time: low beam intensity and high level of contaminating hadronic particles prevented the use of HPGe detectors in this field. Only since the late 1990s, the improvement of beam characteristics permitted to use HPGe crystals, equipped with sophisticated electronics, and to make a spectacular step forward in hypernuclear physics. The energy resolution on low-lying hypernuclear levels was in fact pushed down by almost

three orders of magnitude: from a few MeV, typical value for the current state-of-the-art magnetic spectrometers, to a few keV. A systematic series of experiment were then carried out both at KEK and BNL with Hyperball and Hyperball2, a first and a second generation large acceptance HPGe detector arrays [16, 47–53]. This way it was finally possible to address the central issue of the hypernuclear physics, that is to access to the complete information on the spin-dependence of the $\Lambda \mathcal{N}$ interaction, by looking at the γ-rays following the electromagnetic de-excitation of the studied Λ-hypernuclei ($^{7}_{\Lambda}$Li, $^{9}_{\Lambda}$Be, $^{10}_{\Lambda}$B, $^{11}_{\Lambda}$B, $^{12}_{\Lambda}$C, $^{15}_{\Lambda}$N and $^{16}_{\Lambda}$O). A complete review of this subject can be found in [10].

By following a phenomenological approach [54] the $\Lambda \mathcal{N}$ effective potential can be parameterized in the form expressed by the equation (2.4). Low-lying level energies can be described with radial integrals over the $s_{\Lambda} p_{\mathcal{N}}$ wavefunction [55], usually denoted as $\overline{V}$ (spin-independent interaction), Δ (spin-spin interaction), S_{Λ} (Λ-spin-dependent spin-orbit interaction), $S_{\mathcal{N}}$ (nucleon-spin-dependent spin-orbit interaction) and T (tensor interaction), associated with the V_0, V_σ, V_Λ, $V_{\mathcal{N}}$ and V_T terms in equation (2.4), respectively. The value of Δ, S_{Λ} and T can be experimentally determined by measuring the doublet spacing, while $S_{\mathcal{N}}$ is essentially given by the separation between doublet centroids, that is by the change of the excitation energy of the core nucleus. Then, a fit to the measured hypernuclear excitation spectra finally permits a derivation of the value of the $\Lambda \mathcal{N}$ interaction parameters, as well as of the strength of the $\Lambda - \Sigma$ coupling. Moreover, the determination of the energy level scheme of different Λ-hypernuclei, such as heavy and/or neutron-rich Λ-hypernuclei, offers the opportunity to investigate the effects of $\Lambda \mathcal{N} \mathcal{N}$ three-body force, which originates from the $\Lambda \mathcal{N}$ – $\Sigma \mathcal{N}$ coupling [56, 57] and which cannot be incorporated in the two-body $\Lambda \mathcal{N}$ effective interaction. Such a coupling, besides contributing significantly to doublet spacings in Λ-hypernuclei, has a strong influence on the Λ binding energy in neutron-rich Λ-hypernuclei, as will be discussed in subsection 4.3.

Studies on the spin-dependence of the $s_{\Lambda} p_{\mathcal{N}}$ interaction can be performed as well by looking at the mesonic weak decay spectra, whose analysis makes possible to assign the spin-parity to the decaying hypernucleus (see subsection 5.2). Moreover, the precise measurement of the monochromatic pions emitted in the mesonic weak decay of Λ-hypernuclei at rest provides the most direct measure of Λ binding energies (see subsection 4.3).

3. Historical overview and facilities

The first hyperfragment event was observed in nuclear emulsions in 1952 [32] soon after the discovery of Λ hyperon. In the event, an unusual long-lived nuclear fragment was produced by a high-energy cosmic ray on a nucleus of a photographic emulsion.

3.1. Early emulsion studies

In the early 1960's, K^- beams produced with high-energy proton accelerators were used for hyperfragment production in nuclear emulsions with stopped K^- absorption. In this process, a K^- looses its energy in the target emulsion and it stops to form a kaonic atom with a nucleus (C, N, O, Ag, Br, etc.). The kaonic atom de-excites by emitting X-rays and finally the K^- is absorbed by the nucleus in $K^- \mathcal{N} \to \pi \Lambda / \Sigma$ reactions or $K^- \mathcal{N} \mathcal{N} \to \Lambda / \Sigma \mathcal{N}$ reactions. After the absorption, the Λ is trapped by a nuclear fragment as a hyperfragment. This trapping probability is of the order of

$10^{-4} - 10^{-3}$, so that even with a low K^- beam intensity the hyperfragments were produced abundantly.

The identification of the hyperfragment production was carried out through its weak decay pattern. Namely, the hyperfragment recoils ~ 100 μm in the emulsion before the specific weak decay. When the hyperfragment $^A_\Lambda Z$ decays into $\pi^- + {}^A(Z+1)$, for example, the π^- energy gives us information about the binding energy of the parent hyperfragment. Because of this identification method, the attention was essentially focused on the determination of ground-state binding energies, though some excited-state energies were obtained thanks to the detection of the proton emitted by a hyperfragment [4]. Nevertheless, a systematic measurement from $A = 3$ to $A = 15$ was performed. Also, for several hyperfragments the ground-state spin assignment was carried out by using the mesonic weak decays.

3.2. First counter experiments at CERN PS, BNL AGS and KEK PS

In the 1970's, the so-called recoilless method was successfully utilized in a series of experiments at CERN proton synchrotron (PS) with the in-flight (K^-, π^-) reaction. In this process, the recoil momentum of Λ hyperon is very small (≤ 150 MeV/c) and substitutional states such as (p_n^{-1}, p_Λ) configurations are preferentially excited. Thus, the spectroscopic information of excited states of Λ-hypernuclei were, for the first time, obtained in the missing-mass measurement. A surprisingly small spin-orbit splitting was suggested for the $p-$orbit of Λ-hypernuclei.

From the 1980's to the early 2000's, the Alternating-Gradient Synchrotron (AGS) at BNL and the 12-GeV PS at KEK played very important roles in hypernuclear physics by providing high-intensity K^- and $\pi^\pm$ beams. In this period, the scope of investigations had been extended from Λ-hypernuclei to Σ-hypernuclei, double Λ-hypernuclei and Ξ-hypernuclei, including the $S = -2$ H dibaryon. So, the research field is now called "Strangeness Nuclear Physics", which is more appropriate than "Hypernuclear Physics". Various processes were used to produce a variety of hypernuclei. Not only the (K^-, π^-) reaction but also the (π^+, K^+) and the $(K^-_{\text{stop}}, \pi^{-/0})$ ones were used to produce Λ-hypernuclei in a wide mass number range. The $(K^-, \pi^\pm)$ reactions were also exploited to search for Σ-hypernuclei. In the case of the $S = -2$ systems, the (K^-, K^+) reaction was used. The D6 beam line at BNL-AGS played a unique and important role in studies of the $S = -2$ systems by providing a high-quality and high-intensity K^- beam at 1.8 GeV/c [58].

At KEK-PS, the Superconducting Kaon Spectrometer (SKS) was constructed for the (π^+, K^+) spectroscopy [59]. It had a reasonably good energy resolution of 1.5–2 MeV (FWHM) and a large acceptance of 100 msr. The success was essential to conduct Japanese hypernuclear programs at KEK-PS. Also, the already mentioned Hyperball detector opened a new regime of hypernuclear spectroscopy in precision (a few keV).

3.3. Electro-production of Λ-hypernuclei at JLab Hall A and Hall C

In the 2000s, Thomas Jefferson Laboratory (JLab) started hypernuclear spectroscopy with a different approach, by exploiting the $(e, e'K^+)$ production process.

The first measurement, performed by the E89-009 experiment in Hall C, featured a good energy resolution of 0.8 MeV (FWHM) for the ^{12}C$(e, e'K^+)^{12}_\Lambda$B reaction at ~ 2 GeV [60, 61]. Afterwards, the former Hall C spectrometers for e' and K^+ were

upgraded to High resolution Electron Spectrometer (HES) and High resolution Kaon Spectrometer (HKS) and arranged in a new configuration; this way, in 2005 the E01-011 experiment was able to achieve a $\leq$ 600 keV resolution for the excitation energy spectra of $^{7}_{\Lambda}$He, $^{12}_{\Lambda}$B and $^{28}_{\Lambda}$Al [62]. A further evolution of the experimental setup, aimed to a dramatic suppression of the electromagnetic background and to a substantial increase in luminosity, led to a new series of measurements completed by the E05-115 experiment in 2009 [63]. It was conceived to provide data on $^{7}_{\Lambda}$He with larger statistics and on $^{10}_{\Lambda}$Be, thus offering the opportunity to study it as an $\alpha\alpha n\Lambda$ system in the framework of four-body cluster model calculations [64, 65]. Another important item of its original physics program was the systematic investigation of a wide mass range of Λ-hypernuclei, by using a large set of different targets (^{6}Li, ^{7}Li, ^{9}B, ^{10}B, ^{12}C, ^{51}V, ^{52}Cr and ^{89}Y).

In Hall A, the High Resolution Spectrometer (HRS) electron and hadron arms were used in the E94-107 experiment to measure the $(e, e'K^+)$ reaction at $\sim$4 GeV [41, 66, 67]. Also in this case, a similar sub-MeV resolution was obtained and high-resolution data for $^{12}_{\Lambda}$B, $^{16}_{\Lambda}$N, and $^{9}_{\Lambda}$Li were collected (see subsection 2.5). Such a result was possible thanks to two key technical improvements. From the accelerator side, the higher e^- energy translates in higher virtual photon energy and, finally, in higher K^+ momentum. The resulting longer K^+ flight path before its decay contributes significantly to reduce incident kaon loss in the HRS spectrometer, whose path length is over 20 m. From the experimental apparatus side, the Hall A spectrometer complex was equipped with an innovative proximity focusing Ring Imaging CHerenkov (RICH) [68] and two, newly developed, superconducting septum magnets: the RICH detector provided a cleaner K^+ identification while the additional magnets made possible the detection of extremely forward scattered particles, up to 6 degrees.

3.4. Hypernuclear physics at LNF DAΦNE

FINUDA, Italian acronym for *FIsica NUcleare a DAϕne*, may be classified as a third-generation experiment. It is the paradigm of a hypernuclear physics experiment successfully carried out where it was really hard even to imagine to do it, that is the INFN-LNF Double Annular Φ-factory for Nice Experiments (DAΦNE). Actually an e^+e^- collider was an unconventional playground where to perform such kind of studies that, up to that moment, were essentially carried out at hadron machines, delivering kaon and/or pion beams. Accordingly, the apparatus layout was the one of a fixed-target experiment and the spectrometer had the typical one-arm configuration. What made it so attractive and, ultimately, successful to carry on this project at DAΦNE were the unique and inimitable properties of the K^- mesons following the $\phi(1020)$ resonance disintegration, namely low momentum, substantial monochromaticity, absence of contamination and K^+ correlated emission. Indeed, the low K^- energy (16.1 $\pm$ 0.5 MeV) exploited in an unprecedentedly efficient way the strangeness exchange reaction (K^-, π^-) with stopped K^- in order to produce Λ-hypernuclei on very thin nuclear targets (0.2 - 0.3 g/cm^2). It is important to emphasize that such target thicknesses were lower by one order of magnitude compared to those routinely used in previous fixed-target setups to achieve reasonable event rates. The unmatched advantage of introducing the minimum possible perturbation on the particle momentum to be measured, overcompensates for the low intensity of the K^- source. At the DAΦNE design luminosity of $\mathcal{L} = 1.0 \times 10^{32}$ cm^{-2} s^{-1} the expected

K^+K^- pairs production rate was in fact 2.2×10^2 Hz. The apparatus was then built in the manner of a typical collider apparatus even though it was specially dedicated to an extensive program of hypernuclear physics, mainly focussed on spectroscopy of light Λ-hypernuclei and on systematic study of their decay modes. It was carefully modeled and optimized by means of a sophisticated simulation code, based on the GEANT3 software package [69]. This phase was driven by the constraints imposed by the DAΦNE accelerator's peculiar footprint and by the requirement of fully exploiting both the K^- source topology and the K^- "beam" characteristics. The final outcome was a magnetic spectrometer characterized by a complex architecture, whose complete description can be found in [70].

3.5. Strangeness nuclear physics at J-PARC

The Japan Proton Accelerator Research Complex (J-PARC) [71] has three proton accelerators; a proton linac [72] to inject the proton beam at 400 MeV into a 3-GeV proton synchrotron (PS), the 3-GeV PS [73], operated at 25 Hz with 1 MW beam power, and a 30-GeV main ring (MR) [74] with both slow-extraction and fast-extraction modes. The 3-GeV proton beam is used primarily for materials and life sciences with pulsed neutron and muon beams. The 30-GeV proton beam from the MR is used for particle and nuclear physics experiments in two experimental facilities; the hadron experimental hall and the neutrino beam facility [75]. The beam delivery to these facilities started in 2009. As of June 2014, the achieved maximum beam power delivery was about 230 kW for the neutrino facility and about 20 kW for the hadron experimental hall, which are gradually increasing since 2009.

In the Hadron Experimental Hall [76, 77] there are three beam lines at this moment: K1.8 beam line for medium energy K^- beam up to 2 GeV/c, K_L beam line for neutral kaon rare decays, and K1.1 BR beam line for low momentum K^- beam up to 1.1 GeV/c. The K1.8 beam line was constructed mainly for the $S = -2$ spectroscopy [78]. It has double-stage electro-static separator system to achieve a good K^-/π^- ratio, as in the D6 beam line at BNL, and a beam line spectrometer to carry out the spectroscopic studies with a designed momentum resolution of 0.18% (FWHM). The beam line has a branch option to K1.8BR [79] where the K^- beam up to 1 GeV/c is available with a single-stage electro-static separator. So far, three experiments with pion beams have taken physics data. The first experiment E19 was an experimental search for pentaquark Θ^+ in the $\pi^- + p \rightarrow K^- + X$ reaction at 1.92 GeV/c and 2 GeV/c [80–83]. The second experiment E27 was a search for K^-pp bound state in the $d(\pi^+, K^+)$ reaction at 1.69 GeV/c [84,85] (see subsection 8.2). The third one E10 was a search for a neutron-rich $^6_\Lambda$H hypernucleus (see subsection 4.3).

4. Spectroscopy of single Λ-hypernuclei

4.1. Updated situation on missing-mass spectroscopy

The π^- excitation spectrum obtained at LNF DAΦNE by exploiting the $(K^-_{\mathrm{stop}}, \pi^-)$ reaction, measured on ^{12}C targets with the best achieved energy resolution, revealed new features of relevance for the description of the hypernuclear energy level scheme [86]. Besides the two outstanding peaks, corresponding to the formation of $^{12}_\Lambda$C in the s- and p-states, a sizeable strength for the production of some excited states appears between them. Its overall intensity is of the same order of magnitude of the
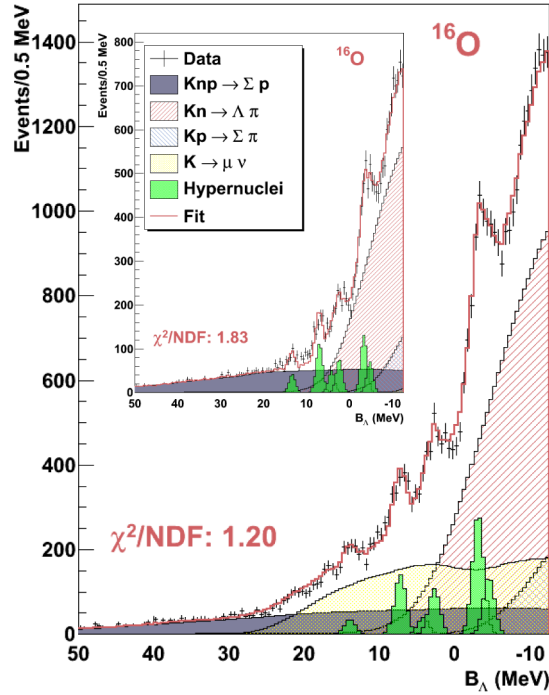
Figure 3. Excitation energy spectrum of $^{16}_{\Lambda}$O obtained with the $(K^-_{\text{stop}}, \pi^-)$ reaction by the FINUDA experiment (from [91]). The inset shows the binding energy distribution for a data sample free from the background due to K^- in flight decay.

one for the production of the $^{12}_{\Lambda}$C ground state $(10^{-3}/K^-_{\text{stop}})$. The importance of such excited nuclear core states was afterwards confirmed, with a better energy resolution, by a measurement carried out at JLab with the $(e, e'K^+)$ reaction on a ^{12}C target [87]. At that time, the observation made by the FINUDA experiment was, to some extent, a surprise: actually, it was not predicted by previous theoretical calculations based on DWIA [88]. However, the presence of two small signals in the region between the two main peaks was also reported in the $^{12}_{\Lambda}$C excitation spectrum obtained at KEK with the (π^+, K^+) reaction [89]. Their measured energy turned out to be (2.6 ± 0.2) MeV and (6.9 ± 0.4) MeV, respectively. Since the position of the second peak was not compatible with the natural interpretation of these structures as states where the ^{11}C excited core and the Λ hyperon in s orbit are weakly coupled, it was conjectured that the state at (6.9 ± 0.4) MeV could be due to an intershell mixing mechanism involving $\Lambda\mathcal{N}$ interaction matrix elements [90].

Stimulated by this observation, the FINUDA Collaboration recently published new data on the spectroscopy of $^{7}_{\Lambda}$Li, $^{9}_{\Lambda}$Be, $^{13}_{\Lambda}$C and $^{16}_{\Lambda}$O, produced by K^- at rest [91]. The observed pattern of excited states is similar to the one obtained with the (π^+, K^+) reaction at 1.05 GeV/c [10]; this fact is not surprising since the two studied reactions are characterized by a comparable momentum transfer ($\sim$300 MeV/c). As an example, the spectrum obtained for the ^{16}O target is reproduced in figure 3. The only significant difference between the two experimental results was the value found for the binding

energy of the $^{16}_{\Lambda}$O ground state, $B_{\Lambda} = (13.4 \pm 0.4)$ MeV, to be compared with the one reported in [10], $B_{\Lambda} = (12.42 \pm 0.05)$ MeV. Despite the larger error, the FINUDA value better agrees with a previous measurement also obtained with stopped K^{-}, $B_{\Lambda} = (12.9 \pm 0.4)$ MeV [92], and with a more recent result achieved with the $(e, e'K^{+})$ reaction on ^{16}O target, leading to the formation of $^{16}_{\Lambda}$N, $B_{\Lambda} = (13.76 \pm 0.16)$ MeV [93]. For these reasons it should be considered more reliable. This statement is now further supported by the recent declaration about the $\sim$0.5 MeV systematic shift that affects all the B_{Λ} values measured at KEK with the SKS spectrometer.

The observed strong dependence on A of the $(K^{-}_{\text{stop}}, \pi^{-})$ capture rates in contrast to the weak one of the (π^{+}, K^{+}) differential cross section is the manifestation of the striking difference in behavior between the strongly attractive K^{-}-nucleus interaction near the threshold and the weakly repulsive K^{+}-nucleus one. This remark represented the starting point for an attempt to determine the value of $\Re(V_{K^{-}})$ [94], quite important for several topics in K-nuclear physics. Different theoretical approaches, varying from shallow potentials at threshold (40–60 MeV) to very deep, density dependent ones (150–200 MeV) were actually proposed. The comparison of the normalized experimental formation rates with the calculations performed with a shallow and, respectively, a deep potential slightly favors the second hypothesis.

4.2. Updated situation on γ-ray spectroscopy

The last experiment dedicated to Λ-hypernucleus γ-ray spectroscopy was performed at KEK in 2005 (E556). E556 measured the $(\pi^{+}, K^{+}\gamma)$ reaction with the SKS spectrometer combined with an upgraded Ge detector, Hyperball2. It observed several γ-transitions in $^{11}_{\Lambda}$B and $^{12}_{\Lambda}$C [95, 96].

Recently, the analysis procedure was improved by paying particular attention to two crucial points: a more accurate correction for the energy loss suffered by final state K^{+} in the thick polyethylene target and a more careful γ-ray energy calibration curve for each Ge crystal [97]. The net result of this effort was an $\sim$10% improvement of the missing-mass energy resolution and then a better signal-to-noise ratio in the mass-gated γ-ray spectrum.

This way, when the mass region for the core-excited s_{Λ} states of $^{12}_{\Lambda}$C (-12 MeV $< -B_{\Lambda} < -2$ MeV) was selected, it was possible to observe four peaks at (161.6 ± 0.2) keV, (2671 ± 3) keV, (2837 ± 4) keV and (6048 ± 6) keV. Once the Doppler-shift correction was applied, the four transition were assigned as $M1(2^{-}_{1} \rightarrow 1^{-}_{1})$, $M1(1^{-}_{2} \rightarrow 2^{-}_{1})$, $M1(1^{-}_{2} \rightarrow 1^{-}_{1})$ and $M1(1^{-}_{3} \rightarrow 1^{-}_{1})$, respectively. While the first three assignments are a welcome confirmation of the previous analysis result [95, 96], the last signal was observed for the first time [16], even though with a limited statistical significance of $\sim 3\sigma$. By taking into account the recoil energy correction to the γ-ray energy, the 1^{-}_{3} state excitation energy turned out to be (6.050 ± 0.006) MeV. Such a value is in a good agreement with the previous determinations provided by E336 [98] and E369 [99] KEK-PS experiments. Also the observed yield of this γ-ray is consistent with the expectation based on the production cross section value measured for the 1^{-}_{3} state by those experiments.

The measured 1^{-}_{3} state excitation energy implies a large negative value for $S_{\mathcal{N}}$ (see subsection 2.5) in contrast with the value of ~ -0.4 MeV [55, 100–102] which reproduces the core excitation energies in $^{7}_{\Lambda}$Li, $^{15}_{\Lambda}$N and $^{16}_{\Lambda}$O. This situation is completely analogous to the $^{12}_{\Lambda}$C($1^{-}_{2}, 1^{-}_{1}$), $^{11}_{\Lambda}$B($1/2^{+}, 5/2^{+}$) and $^{13}_{\Lambda}$C($3/2^{+}, 1/2^{+}$) cases whose interpretation requires a large negative $S_{\mathcal{N}}$ value as well.

4.3. Neutron-rich Λ-hypernuclei

A neutron-rich Λ-hypernucleus is a bound strange nuclear system with an unbalanced number of constituent neutrons or, in other words, with an unusually high neutron to proton ratio [103]. The search for such systems is legitimated by the experimental observation of the so-called glue-like role that the Λ hyperon manifests when is embedded in a nucleus [46]. This property is essentially due to the attractive nature of the $\Lambda\mathcal{N}$ interaction and to the fact that the Pauli principle is not effective for a single strange particle inside a nucleus. Unstable nuclear systems, like for instance ^{8}Be, become then particle stable thanks to the critical contribution to the overall binding energy carried by the Λ. This effect is particularly evident for nuclei close to the proton- and neutron-drip lines, thus potentially expanding the boundary of the nuclear stability valley.

The motivations for trying to observe and for studying neutron-rich Λ-hypernuclei span over a wide spectrum. The discovery of these exotic systems could open very interesting scenarios as far as the investigation of few-body nuclear systems and of $\Lambda\mathcal{N}$ interactions (both strong and weak) in low density nuclear medium are concerned. This environment is then best suited to investigate the effects of the three-body forces involving hyperons ($\Lambda\mathcal{N}\mathcal{N}$) which are believed to be repulsive at short range and to recover the stiffness of the nuclear matter EoS with hyperons in neutron stars [104,105]. In this respect, a precise knowledge of light neutron-rich Λ-hypernuclei energy level structure could imply far-reaching consequences on strange dense stellar matter properties. Indeed, by constraining the $\Lambda\mathcal{N}$ potential it could be possible to make more reliable predictions about the internal structure of neutron stars and in particular about their mass maximum value [106]. However, the recent measurements of two neutron star masses with values of the order of 2 $M_\odot$ [30, 107] seriously questions the real presence of hyperons in the neutron star core composition [108]. A possible way to face with this "hyperon crisis" is an extension of the three-body forces definition, by including the additional $YY\mathcal{N}$ and YYY channels as well. This way it would be possible to provide enough repulsive strength at high density stellar matter, thus partially recovering the stiffness of the EoS and then justifying the observation of very massive neutron stars.
When focusing the attention on the strict hypernuclear physics field, such studies offer the opportunity to evaluate the strength of the $\Lambda\mathcal{N}$ – $\Sigma\mathcal{N}$ coupling by tuning microscopic shell-model calculations to reproduce the structure of the observed neutron-rich Λ-hypernuclei [109–113] and to check whether such a mechanism is able to generate a sizeable attraction for specific spin-isospin channels [114–119].

The existence and the observability of neutron-rich Λ-hypernuclei were first discussed by Dalitz and Levi Setti [103]. Afterwards, Majling endorsed this hypothesis and provided even more stringent predictions about their production rates [120].

In s- and p-shell Λ-hypernuclei, particle-stable states consist typically of a Λ in $1s$-shell coupled to a nuclear core. Hence, as already recalled, the total binding energy of the system is generally increased to a significant extent with respect to the core nucleus. This way, initially unstable nuclear cores can be made bound and it is possible to observe stable Λ-hypernuclei corresponding to unbound core systems. Experimental evidences were actually found for $^6_\Lambda$He, $^7_\Lambda$Be, $^8_\Lambda$He, $^9_\Lambda$Be and $^{10}_\Lambda$B hypernuclei in emulsion experiments [121]. However, no unstable-core hydrogen Λ-hypernuclei were observed until very recently. $^6_\Lambda$H is the simplest neutron-rich hypernucleus and, at the same time, it is the bound strange nuclear system with the largest possible neutral baryon

excess. Actually it would be $(N + Y)/Z = 5$, with $Y = 1$ for a Λ hyperon, or $N/Z = 4$, larger than the maximal value in light nuclei $N/Z = 3$ for ^{8}He [122]. In this case the stabilized core nucleus is ^{5}H.

The accelerator-aided neutron-rich Λ-hypernucleus production can be achieved by exploiting the two-body double charge-exchange reaction

$$K^- + {}^A Z \to {}^A_\Lambda (Z - 2) + \pi^+, \tag{4.1}$$

induced on nuclear targets by K^- meson both in flight and at rest, or

$$\pi^- + {}^A Z \to {}^A_\Lambda (Z - 2) + K^+ \tag{4.2}$$

with π^- mesons in flight ($p_{\pi^-} > 0.89$ GeV/c).
Both these reactions can be described as two-step processes involving two different protons of the same nucleus, in which they are sequentially transformed into a Λ particle and a neutron (or vice versa), leading to a final bound strange nuclear system. Another possible mechanism could be a one-step double charge exchange $m_i^- p \to \Sigma^- m_f^+$ (where m_i^- stands for the initial π^-/K^- meson and m_f^+ for the final K^+/π^+ one) feeding the Σ component coherently admixed into the final Λ hypernuclear state. The two-step processes (4.1) and (4.2) are expected to occur at a rate two orders of magnitude smaller [123] than the ones for "normal" Λ-hypernuclei production via the corresponding one-step two-body reactions (K^-, π^-) and (π^+, K^+).

The first experimental attempt to produce neutron-rich hypernuclei was carried out by exploiting the reaction (4.1) at KEK [124]. Upper limits were obtained for the production of $^9_\Lambda$He, $^{12}_\Lambda$Be and $^{16}_\Lambda$C (on ^{9}Be, ^{12}C and ^{16}O targets respectively), all lying in the $(0.6 - 2.0) \times 10^{-4}/K^-_{\text{stop}}$ range. A second KEK experiment (E521), reported the production of $^{10}_\Lambda$Li in the (π^-, K^+) reaction on a ^{10}B target using a 1.2 GeV/c π^- beam, with a cross section of (11.3 ± 1.9) nb/sr, integrated over the whole Λ bound region [125].

The FINUDA Collaboration pursued the objective of producing and of detecting $^6_\Lambda$H, $^7_\Lambda$H and $^{12}_\Lambda$Be since the very beginning of its activity, by exploiting the unrivaled characteristics of the kaon source available at DAΦNE jointly to the excellent performances of the apparatus.

The strategy adopted in analyzing the first limited data sample ($\mathcal{L}_{\text{int}} \sim 220$ pb^{-1}) consisted in searching for discrete peaks in the region of interest in the momentum spectrum of π^+ emitted following the K^- capture at rest on ^{6}Li, ^{7}Li and ^{12}C targets. Because of the overwhelming background due to concurrent K^- induced processes, it was possible to provide only upper limits at a 90% C.L., namely $R_{\pi^+} \left({}^6_\Lambda \text{H} \right) \leq \left(2.5 \pm 0.4 \,_{\text{stat}} \,^{+0.4}_{-0.1} \,_{\text{syst}} \right) \times 10^{-5}/K^-_{\text{stop}}$, $R_{\pi^+} \left({}^7_\Lambda \text{H} \right) \leq \left(4.5 \pm 0.9 \,_{\text{stat}} \,^{+0.4}_{-0.1} \,_{\text{syst}} \right) \times 10^{-5}/K^-_{\text{stop}}$ and $R_{\pi^+} \left({}^{12}_\Lambda \text{B}e \right) \leq \left(2.0 \pm 0.4 \,_{\text{stat}} \,^{+0.3}_{-0.1} \,_{\text{syst}} \right) \times 10^{-5}/K^-_{\text{stop}}$ respectively [126]. In the case of $^{12}_\Lambda$Be, the FINUDA determination lowered by a factor $\sim$3 the aforementioned KEK results [124].

A second data taking campaign increased the statistics collected with ^{6}Li targets by a factor 5 ($\mathcal{L}_{\text{int}} \sim 1156$ pb^{-1}). However even in this case it was not possible to observe in the inclusive π^+ momentum spectrum clear peaks that could be unambiguously attributed to the two-body, double charge exchange reaction:

$$K^-_{\text{stop}} + {}^6\text{Li} \to {}^6_\Lambda \text{H} + \pi^+ \quad (p_{\pi^+} \approx 252 \text{ MeV}/c \text{ when } B_\Lambda \approx 5 \text{ MeV}). \tag{4.3}$$

Then, by exploiting the larger number of reconstructed events, a new analysis strategy was adopted with the aim of reducing the physical background. It consisted in looking

Table 1. Pion momenta $p_{\pi\pm}$ and mass values for the three $^6_\Lambda$H candidate events. Masses are evaluated both from production (4.3) and decay (4.4) reactions. In the last two columns the mass mean value and the difference between production and decay masses are reported (from [128]).

p_{π^+} [MeV/c]	p_{π^-} [MeV/c]	M($^6_\Lambda$H) prod. [MeV]	M($^6_\Lambda$H) decay [MeV]	M($^6_\Lambda$H) mean [MeV]	ΔM($^6_\Lambda$H) [MeV]
251.3 ± 1.1	135.1 ± 1.2	5802.33 ± 0.96	5801.41 ± 0.84	5801.87 ± 0.96	0.92 ± 1.28
250.1 ± 1.1	136.9 ± 1.2	5803.45 ± 0.96	5802.73 ± 0.84	5803.09 ± 0.96	0.72 ± 1.28
253.8 ± 1.1	131.2 ± 1.2	5799.97 ± 0.96	5798.66 ± 0.84	5799.32 ± 0.96	1.31 ± 1.28

at the π^+ momentum distribution by requiring in coincidence the π^- coming from the $^6_\Lambda$H mesonic decay:

$$^6_\Lambda\text{H} \rightarrow {}^6\text{He} + \pi^- \qquad (130 \leq p_{\pi^-} \leq 140 \text{ MeV}/c). \qquad (4.4)$$

Three events, out of the 27×10^6 ones due to K^- stopped in the two ^{6}Li targets, survived to the filtering procedure [127], described in detail in [128]. The $^6_\Lambda$H mass values evaluated for each event both from production (4.3) and decay (4.4) processes are listed in table 1; the quoted errors are evaluated directly from the tracker momentum resolution for π^+ and π^-. Such nuclear mass values yield a mean value $M(^6_\Lambda\text{H}) = (5801.4 \pm 1.1)$ MeV where the error is essentially due to the spread of the average mass values for the three events. The inferred $^6_\Lambda$H binding energies $B_\Lambda = (4.0 \pm 1.1)$ MeV, with respect to the ($\Lambda + {}^5$H) threshold, and $B_\Lambda = (0.3 \pm 1.1)$ MeV, with respect to the lowest particle stable threshold ($^4_\Lambda$H + 2n), are in excellent agreement with the predictions of both [103] and [120]. On the contrary the first value is significantly lower than the outcome of the calculations described in [114–119], where the coherent $\Lambda\mathcal{N}$-$\Sigma\mathcal{N}$ coupling effect is invoked in order to justify a considerable higher binding energy for $^6_\Lambda$H. Then the present result seems to support the hypothesis of a reduced effectiveness of such a mechanism, in line with the output of some recent shell-model calculations [55, 131].

The mass values obtained from production process (4.3) turned out to be systematically higher than those inferred from decay one (4.4) by (0.98 ± 0.74) MeV. A possible physical origin for such a difference, discussed in [127] and [128], could be related to the $^6_\Lambda$H excitation spectrum: the production could occur preferentially to an ~ 1 MeV 1^+ excited state, then decaying through a fast (undetected) M1 γ-transition to the 0^+ ground state of $^6_\Lambda$H, which in turn undergoes the mesonic weak decay.

In order to provide a correct evaluation of the $^6_\Lambda$H production rate, a careful study of the possible background sources was performed. A complete simulation of K^-_{stop} absorption reactions, both on single and on correlated few-nucleons clusters, leading to the formation and the decay of Λ and Σ hyperons was then carried out. The full description of this task can be found in [128]. The evaluated total number of events due to both physical and instrumental background was found to be (0.43 ± 0.28). Thus, by using Poisson statistics, it was possible to conclude that the three $^6_\Lambda$H-assigned events do not arise from background at a 99% confidence level, the statistical significance of the result being S = 3.9. Taking into account the above considerations, the apparatus reconstruction efficiency for $\pi^\pm$, the target purity and the selection cut effectiveness

the product $R_{\pi+} \cdot \mathrm{BR}(\pi^-)$, where $R_{\pi+}$ is the $^6_\Lambda\mathrm{H}$ production rate per K^-_stop in reaction (4.3) and $\mathrm{BR}(\pi^-)$ is the unknown branching ratio for the two-body mesonic π^- decay (4.4), turned out to be:

$$R_{\pi+}(^6_\Lambda\mathrm{H}) \cdot BR(\pi^-) = (2.9 \pm 2.0) \times 10^{-6}/K^-_\mathrm{stop}. \tag{4.5}$$

Finally, by assuming $\mathrm{BR}(\pi^-) = 49\%$, in analogy to the experimental result for $^4_\Lambda\mathrm{H} \rightarrow {}^4\mathrm{He} + \pi^-$ decay [129], $R_{\pi+}(^6_\Lambda\mathrm{H}) = (5.9 \pm 4.0) \times 10^{-6}/K^-_\mathrm{stop}$, a value fully consistent with the previous published result [126] and two to three orders of magnitude smaller than summed Λ-bound production rates $R_{\pi-}$ of "normal" light Λ-hypernuclei in the $(K^-_\mathrm{stop}, \pi^-)$ reaction [91].

The FINUDA claim is now triggering a lively debate on the $^6_\Lambda\mathrm{H}$ existence and its structure in both the theoretical and in the experimental physics communities. Very recently, Hiyama *et al.* computed the $^6_\Lambda\mathrm{H}$ binding energy by exploiting a four-body cluster-model [130]. According to these calculations, which are able to reproduce the $^5\mathrm{H}$ properties, the Λ separation energy amounts to $B_\Lambda = 2.47$ MeV only. This means that both 0^+ and 1^+ states are unbound, in contrast to the FINUDA experimental evidence. Gal and Millener performed a shell-model calculation in order to predict in turn the binding energy for the system made by a $^4_\Lambda\mathrm{H}$ core plus a pair of neutrons [131]. In this case the obtained binding energy value was $B_\Lambda = (3.83 \pm 0.08 \pm 0.22)$ MeV, thus leaving room for an alternative interpretation of the FINUDA observation. They suggested that the 1^+ excited state could be unbound but characterized by a particle decay width extremely small and comparable with the one of the aforementioned M1 γ-transition to the 0^+ ground state. Such a hypothesis could be justified on the basis of a kinematical and dynamical suppression of the two neutron emission from the 1^+ state.

From the experimental point of view, it is clear that the $^6_\Lambda\mathrm{H}$ discovery must be confirmed in an independent way and with much higher statistical significance. In this perspective, the E10 experiment was proposed and approved to run on the K1.8 beam line at J-PARC. It has been specifically designed to search for neutron-rich Λ-hypernuclei, namely $^6_\Lambda\mathrm{H}$ and $^9_\Lambda\mathrm{He}$, and it could be considered the natural extension of the already mentioned KEK E521 one [125]. Actually, the neutron-rich Λ-hypernucleus production reaction exploited is the process (4.2) at 1.2 GeV/c. The E10 Collaboration took data in December 2012 and January 2013 with a $^6\mathrm{Li}$ target. The careful analysis of the measured missing mass spectrum found no significant indication for $^6_\Lambda\mathrm{H}$ existence, neither below nor above the $(^4_\Lambda\mathrm{H} + 2\mathrm{n})$ particle decay threshold [132]. On the basis of three observed events in the region of interest, an upper limit for the production cross section of a bound $^6_\Lambda\mathrm{H}$ hypernucleus was estimated to be 1.2 nb/sr at a 90% C.L., a value one order of magnitude lower that the one reported in the analogous KEK measurement on $^{10}\mathrm{B}$ target [125].

FINUDA looked for $^9_\Lambda\mathrm{He}$ as well by applying the same analysis strategy described above to a sample of events induced by stopped K^- on a $^9\mathrm{Be}$ target, that is by searching for $\pi^+\pi^-$ pairs in coincidence from the neutron-rich Λ-hypernucleus production process

$$K^-_\mathrm{stop} + {}^9\mathrm{Be} \rightarrow {}^9_\Lambda\mathrm{He} + \pi^+ \quad (p_{\pi+} \approx 257.5 \text{ MeV}/c \text{ when } B_\Lambda \approx 8.5 \text{ MeV}) \tag{4.6}$$

and, respectively, from its following mesonic decay

$$^9_\Lambda\mathrm{He} \rightarrow {}^9\mathrm{Li} + \pi^- \qquad (p_{\pi-} \approx 117 \text{ MeV}/c). \tag{4.7}$$

This time no event satisfied the selection cuts. Then, only an upper limit was provided for the $^9_\Lambda\mathrm{He}$ production, amounting to $1.6 \times 10^{-5}/K^-_\mathrm{stop}$ at 90% C.L. [133]. Also

in this case, such a determination improved by more than one order of magnitude the previous result obtained at KEK [124]. Unfortunately, it should be noted that, despite the remarkable effectiveness of the decay pion coincidence measurement, this method has not a general validity: indeed it was not possible to apply it in order to search for $^7_\Lambda$H because its daughter nucleus ^{7}He produced in the two-body weak decay $^7_\Lambda$H $\to$ ^{7}He $+ \pi^-$ is particle-unstable.

Another important and recently achieved experimental result is the $^7_\Lambda$He neutron-rich hypernucleus observation by the ^{7}Li$(e, e'K^+)^7_\Lambda$He reaction. The JLab Hall C Collaboration succeeded in extracting from a huge background the signal corresponding to the formation of the $^7_\Lambda$He $1/2^+$ ground state [134]. A pilot measurement, E89-009, was first performed at JLab in 2000 in order to verify the feasibility of $^AZ(e, e'K^+)^A_\Lambda(Z - 1)$ hypernuclear spectroscopy [60, 61]. The experiment demonstrate that ^{12}C$(e, e'K^+)^{12}_\Lambda$B spectroscopy with sub-MeV resolution was possible, thanks to the JLab high quality electron beam and the spectrometer system performance. Its natural extension was then the E01-011 experiment, carried out in 2005. The measured value for the Λ binding energy was $B_\Lambda = (5.68 \pm 0.03_{\text{stat}} \pm 0.25_{\text{syst}})$ MeV while the virtual photon differential cross section turned out to be $\overline{\frac{d\sigma}{d\Omega}} = (26.0 \pm 5.1_{\text{stat}} \pm 9.9_{\text{syst}})$ nb/sr. The Hall C Collaboration observation is in qualitatively good agreement with a previous result obtained in an emulsion experiment [121], because no $^7_\Lambda$He ground state mass value was reported in literature due to the low statistics and low quality former measurements.

These observations are not only important in themselves, but they provide as well a new input to the discussion on a possible charge symmetry breaking (CSB) effect of the $\Lambda\mathcal{N}$ potential. Actually, $^7_\Lambda$He was the missing member of the $A = 7$, $T = 1$ isospin triplet, the other two being $^7_\Lambda$Li* and $^7_\Lambda$Be. As noticed by Hiyama *et al.* [135], this isotriplet is the ideal testing ground to look for CSB effect manifestation. The Λ separation energy for each member of the isotriplet was then evaluated using a four-body cluster model explicitly taking into account the CSB effect. Indeed, a $\Lambda\mathcal{N}$ CSB potential was phenomenologically introduced to account for the measured Λ binding energy difference between the $^4_\Lambda$H and $^4_\Lambda$He mirror Λ-hypernuclei belonging to the $A = 4$, $T = 1/2$ isodoublet. Accurate Faddeev-Yakubovsky calculations performed for $^4_\Lambda$H and $^4_\Lambda$He Λ-hypernuclei [136] confirmed that the introduction of a sizeable CSB effect is fully justified, though the role played by the Coulomb force in determining the difference between the Λ separation energies of the 0^+ ground and the 1^+ excited states of the two hypernuclear systems turned out to be significantly downsized with respect to the previous estimation given in [137]. As a matter of fact, the gaps $B_\Lambda\left(^4_\Lambda\text{He}\right) - B_\Lambda\left(^4_\Lambda\text{H}\right) = (0.35 \pm 0.06)$ MeV, for the 0^+ ground state, and $B_\Lambda\left(^4_\Lambda\text{He}\right) - B_\Lambda\left(^4_\Lambda\text{H}\right) = (0.24 \pm 0.06)$ MeV, for the 1^+ excited state, remain surprisingly large even after applying the corrections due to the Coulomb interaction [138]. However, the outcome of the calculation performed for all the $A = 7$, $T = 1$ isotriplet members seems to indicate that no explicit CSB contribution is required in order to reproduce the experimental results.

5. Weak Decay of single Λ-hypernuclei

Ordinary matter doesn't explicitly contain strangeness. Then, the fate of a hypernucleus is to decay to ordinary matter with a lifetime comparable, to a first approximation, to the embedded hyperon lifetime. In-medium weak decays of

hyperons offers a unique tool for investigating elusive aspects of the weak interaction, that would otherwise remain inaccessible. This is in particular true for non-mesonic, one-nucleon induced $\Lambda\mathcal{N} \to \mathcal{N}\mathcal{N}$ and two-nucleon induced $\Lambda\mathcal{N}\mathcal{N} \to n\mathcal{N}\mathcal{N}$ processes that can occur only inside a nucleus. The most suitable environment for such studies is the Λ-hypernucleus: being the lightest hyperon, the Λ can actually decay only through weak processes. Besides this intrinsic interest, the Λ-hypernucleus decay study represents a powerful discovery tool which led to several other results, sometimes unexpected. A Λ-hypernucleus can be produced either in its ground state or in an excited state of the Λ-particle neutron-hole configuration. When the system is excited beyond the particle emission threshold, it decays dominantly by strong interaction by emitting either single nucleons or nuclear fragments; the residual strange nuclear fragment then reaches its ground state through electromagnetic transitions. Finally, a Λ-hypernucleus in its ground state decays to non-strange nuclear systems through the mesonic (MWD) or the non-mesonic (NMWD) weak decay channel.

In the hypernucleus MWD the Λ decays into a nucleon and a pion like it does in free space

$$\begin{aligned} {}_{\Lambda}^{A}Z \to {}^{A}(Z+1) + \pi^- \qquad &(\Lambda_{\text{free}} \to p + \pi^- + 37.8 \text{ MeV}), \qquad &(5.1a)\\ {}_{\Lambda}^{A}Z \to {}^{A}Z + \pi^0 \qquad &(\Lambda_{\text{free}} \to n + \pi^0 + 41.1 \text{ MeV}). \qquad &(5.1b) \end{aligned}$$

When this process occurs at rest, the outgoing nucleon carries a momentum $q \approx 100$ MeV, that corresponds to Q-value of about 40 MeV. The measured branching ratios of the channels (5.1a) and (5.1b) are consistent with the empirical $\Delta I = 1/2$ rule, valid for all non-leptonic, strangeness-changing, processes, like the Σ hyperon decay and the K pionic decays. When a Λ hyperon is embedded in a hypernucleus, the increase of its binding energy ($\sim$3 MeV for ${}_{\Lambda}^{5}$He, $\sim$11 MeV for ${}_{\Lambda}^{12}$C, $\sim$27 MeV for ${}_{\Lambda}^{208}$Pb) further reduces the energy available to the final-state particles; the MWD channel is thus suppressed in hypernuclei with respect to the free-space decay due to the Pauli principle, since the emitted nucleon momentum is by far smaller than the nuclear Fermi momentum ($k_F \approx 270$ MeV/c) in all nuclei except the lightest, s-shell ones.

The observation of the hypernucleus NMWD is one of the most striking manifestations of the so called medium effect. In fact such a decay mode has not an analogue for a free Λ and it can occur inside nuclear matter only. Indeed this interaction involves the hyperon and one core nucleon. Its relevance was pointed out soon after the first discovery of a Λ-hypernucleus [139]. It was explained by assuming that the pion emitted in the weak vertex $\Lambda \to \pi\mathcal{N}$ is virtual and it is then absorbed by the nuclear medium, resulting in one of the following processes:

$$\begin{aligned} {}_{\Lambda}^{A}Z \to {}^{(A-2)}(Z-1) + n + p \qquad &(\Lambda + p \to n + p + \sim 175 \text{ MeV}), \qquad &(5.2a)\\ {}_{\Lambda}^{A}Z \to {}^{(A-2)}Z + n + n \qquad &(\Lambda + n \to n + n + \sim 175 \text{ MeV}). \qquad &(5.2b) \end{aligned}$$

Such processes are four-fermion, $\Delta S = 1$, baryon-baryon weak interactions and they represent the only practical way to obtain information on the weak vertex $\Lambda\mathcal{N} \to n\mathcal{N}$, which represents the first extension of the weak, $\Delta S = 0$, $\mathcal{N}\mathcal{N} \to \mathcal{N}\mathcal{N}$ interaction to the strange baryon sector. It is worthwhile to remember that the short Λ lifetime prevents the use of hyperon targets or of beams of suitable intensity: only scarce $\Lambda\mathcal{N}$ scattering data are then presently available. Moreover, processes (5.2a) and (5.2b) are the best testing ground to investigate the parity-conserving part of the weak interaction, which is completely masked by the strong one in the $\mathcal{N}\mathcal{N} \to \mathcal{N}\mathcal{N}$ [140–142].

Some inconsistencies and some difficulties in the interpretation of the experimental data on the Λ-hypernucleus decay, like for instance the so called Γ_n/Γ_p puzzle [143–145], led to speculation that sometimes the virtual pion from the Λ decay process can be absorbed by a pair of core nucleons (np, pp or nn), correlated by the strong interaction [146], according to the following reactions:

$$^A_\Lambda Z \rightarrow {}^{(A-3)}(Z-1) + n + n + p \qquad (\Lambda + np \rightarrow n + n + p + \sim 175 \text{ MeV}), \quad (5.3a)$$
$$^A_\Lambda Z \rightarrow {}^{(A-3)}(Z-2) + n + p + p \qquad (\Lambda + pp \rightarrow n + p + p + \sim 175 \text{ MeV}), \quad (5.3b)$$
$$^A_\Lambda Z \rightarrow {}^{(A-3)}Z + n + n + n \qquad (\Lambda + nn \rightarrow n + n + n + \sim 175 \text{ MeV}). \quad (5.3c)$$

These three decay channels have different widths and, according to a microscopic calculation [147], the so called two-nucleon induced decay is largely dominated by the (5.3a) one. Then, very often the np-induced channel width Γ_{np} is assumed to be equivalent to the total two-nucleon induced process width $\Gamma_{2\mathcal{N}}$.

Like in the case of one-nucleon induced NMWD, these decay modes can take place only in nuclei; the Q-value of their corresponding elementary reaction (indicated in parentheses in (5.3a)-(5.3c)) is $\sim$175 MeV and then it is high enough to overcome any Pauli blocking effect. Indeed, the outgoing nucleon momenta are as high as $\sim$420 MeV/c, in the one-nucleon induced process, and $\sim$340 MeV/c in the two-nucleon induced one, provided that the available energy is equally divided among all the final-state particles: this way the outgoing nucleons have a great probability to escape from the parent nucleus. For this reason, the NMWD channel dominates over the MWD one for all but the s-shell Λ-hypernuclei and only for very light systems (A $\leq$ 5) the two decay modes are competitive.

The experimental quantities that can be directly measured by observing hypernuclear decays are: the hypernucleus lifetime $\left(\tau\left({}^A_\Lambda Z\right)\right)$; the branching ratios and the decay rates for the MWD channels (5.1a) and (5.1b) (Γ_{π^-} and Γ_{π^0}, respectively); the kinetic energy distributions for light decay products (pions and nucleons) from both MWD and NMWD processes. On the contrary, the overall NMWD rate can be only determined in an indirect way as $\Gamma_{\text{NMWD}} = \Gamma_{\text{total}} - \Gamma_{\text{MWD}}$. As a matter of fact, it is not possible to directly determine the partial decay rates for the NMWD channels (5.2a)-(5.3c) (Γ_p, Γ_n, Γ_{np}, Γ_{pp}, Γ_{nn}, respectively) due to the not negligible distortion introduced by the Final State Interaction (FSI) suffered by nucleons from weak decay.

A survey of the experimental results achieved and of the theoretical models developed to describe the hypernuclear weak decay up to 1990 can be found in [148]; recent updates are given in review papers [11, 140–142, 149].

5.1. Λ-hypernucleus lifetime

Among the experimental observables, $\tau\left({}^A_\Lambda Z\right)$ is the one that can be measured with the highest accuracy, being unaffected by all the distortions due to FSI suffered by decay products. The first determination dates back to the 60s. Since then, several measurements were performed by resorting to a large variety of different experimental approaches: photographic emulsions [150–154], LH$_2$ filled bubble chambers [155–157], counter experiments [143, 158–164], heavy ion collision [165], electro-production [166], low-momentum $\bar{p}A$ annihilations [167, 168], pA collisions [169]. It is worth noting that not all the listed techniques were able to provide the decay timing, then sometimes only indirect $\tau\left({}^A_\Lambda Z\right)$ determinations were possible. The obtained results span over a large target A interval ranging from ^{3}H to ^{238}U. When plotted against Λ-hypernuclei mass number, $\tau\left({}^A_\Lambda Z\right)$ values, that for low A systems are compatible within the error

with the free Λ lifetime, appear quite stable in passing from low to medium A, while starting from $A = 20$ they first decrease and then they level off around 210 ps, that is $\sim 80\%$ of free Λ lifetime (see [162]). Such a trend is understood in terms of the anticorrelation between the MWD and NMWD modes: the rapid decrease of the MWD amplitude seems to be compensated by the increase of the NMWD one; in addition the medium A asymptotic behavior suggests the presence of saturation properties for the $\Lambda \mathcal{N} \rightarrow n \mathcal{N}$ weak interaction, analogous to those of the finite range $\mathcal{N} \mathcal{N}$ strong interaction. The only exception was the outcome of the first experiment where hypernuclei were produced via heavy ion collisions. Even though it was not possible to identify them, their lifetime was extracted from the recoil distance distribution and it turned out to be $\tau \left({}^{16}_{\Lambda} Z \right) \approx 96$ ps [165], a value surprisingly small that, owing to the experimental method limitations, was however considered not reliable.

Similar questions arose when lifetime of high A hypernuclear systems were indirectly inferred from low-momentum $\bar{p}A$ annihilations studied at CERN and from pA collisions observed at COSY. Actually, $\bar{p}A$ experiments provided $\tau \left({}^{A}_{\Lambda} Z \right)$ values of the order of (180 ± 40) ps and of (130 ± 30) ps on the basis of the measurements performed on ^{209}Bi [167] and ^{238}U [168] targets, respectively; equally short lifetimes were determined from pA collisions, namely (130 ± 20) ps, (161 ± 16) ps and (138 ± 18) ps on ^{197}Au, ^{209}Bi and ^{238}U targets, respectively [169]. Also in these cases, some doubts about the results exist owing to the fact that it was not possible to identify the decaying hypernuclear system and that lifetime value determination crucially relies on calculated, model dependent, A, Z and velocity distributions, which take into account the interaction dynamics during the whole time evolution of the process. If confirmed, such low values could suggest a very different behavior of the Λ when embedded in massive nuclei, where its interaction with the core nucleons seems to be stronger and to involve a large fraction of them. The complexity of the system may provide room for unknown interaction mechanism which could open beyond some A threshold value (> 60) and could explain the strong enhancement of the interaction strength for $A > 180$.

Even more puzzling is the recent claim of the STAR Collaboration about the lifetime of ${}^{3}_{\Lambda}$H and ${}^{3}_{\Lambda}\overline{\text{H}}$, produced in Au + Au collisions at $\sqrt{s_{NN}} = 200$ GeV [170]. The measured value, obtained by combining the candidate ${}^{3}_{\Lambda}$H and ${}^{3}_{\Lambda}\overline{\text{H}}$ samples, turned to be $\tau \left({}^{3}_{\Lambda}\text{H} \right) = \left(182^{+89}_{-45}\,_{\text{stat}} \pm 27\,_{\text{syst}} \right)$ ps, a value significantly lower than the one obtained in direct measurements but still compatible with the free Λ particle within the uncertainties. A subsequent analysis of a STAR larger data sample led to an even shorter (anti)hypertriton lifetime $\tau \left({}^{3}_{\Lambda}\text{H} \right) = \left(123^{+26}_{-22}\,_{\text{stat}} \pm 10\,_{\text{syst}} \right)$ ps [171].

Such a result was confirmed by another recent experiment where ${}^{3}_{\Lambda}$H and ${}^{4}_{\Lambda}$H hypernuclei were produced at GSI by driving a ^{6}Li beam on a ^{12}C target at 2 A GeV [172]. The HypHI Collaboration, which by the way has the merit of having demonstrated the feasibility of hypernuclear spectroscopy with heavy-ion beams, provided a value for ${}^{3}_{\Lambda}$H lifetime in agreement with the first STAR one, namely $\tau \left({}^{3}_{\Lambda}\text{H} \right) = \left(183^{+42}_{-32}\,_{\text{stat}} \pm 37\,_{\text{syst}} \right)$ ps, while the determination for ${}^{4}_{\Lambda}$H led to $\tau \left({}^{4}_{\Lambda}\text{H} \right) = \left(140^{+48}_{-33}\,_{\text{stat}} \pm 35\,_{\text{syst}} \right)$ ps.

Undoubtedly these further hypernucleus lifetime values in contrast with the trend of the previous measurements, obtained in emulsion and/or bubble chamber experiments [162], should trigger a critical discussion on the available results and a dedicated experimental effort to clarify the situation.

5.2. Mesonic weak decay

Since the first experiments performed with photographic emulsions, the study of MWD has produced important information about Λ-hypernuclei. By applying the newly established features of the free Λ mesonic decay ($\Delta I = 1/2$ rule; dominance of the s-wave, parity-violating, spin-non-flip amplitude; π angular distribution dependence on Λ spin axis) to a Λ embedded in a bound nuclear system it was possible to extract ground-state spin and parity values for several Λ-hypernuclei: $^3_\Lambda$H, $^4_\Lambda$H, $^4_\Lambda$He, $^8_\Lambda$Li, $^{11}_\Lambda$B and $^{12}_\Lambda$B [173–179].

Thanks to the development of the counter experiment technique, applied to the study of Λ-hypernuclei produced by (K^-, π^-) and (π^+, K^+) reactions, a remarkable amount of experimental results on Γ_{π^-} and Γ_{π^0} is today available in literature for light Λ-hypernuclei up to $^{15}_\Lambda$N [143, 159, 160, 163, 180, 181]. Comprehensive calculations of the main physical features of MWD were successfully carried out for s-shell [182, 183], p-shell [183–185] and sd-shell [183, 185] exploiting large data sets collected essentially at KEK. Nevertheless, MWD still attracts lively interest: as a matter of fact the observation of such a process, in which a pion is created by the Λ hyperon decay deep inside a nucleus, offers a unique opportunity to investigate in-medium pion properties and to discriminate among different off-shell extrapolations inherent in potential models.

One of the most recent systematic studies on hypernuclear MWD was performed by the FINUDA Collaboration, which looked at the charged decay channel (5.1a) of $^5_\Lambda$He and of several p-shell hypernuclei, namely $^7_\Lambda$Li, $^9_\Lambda$Be, $^{11}_\Lambda$B and $^{15}_\Lambda$N [181]. The innovative aspect of these FINUDA measurements is due to the fact that up to that moment all the available information consisted essentially of $\Gamma_{\pi^-}/\Gamma_\Lambda$ and $\Gamma_{\pi^0}/\Gamma_\Lambda$ ratio compilations. Such values were obtained thanks to counting experiments in which decay pions are just detected in coincidence with hypernucleus formation π^- (see (2.5a)), without any magnetic analysis. Actually, π^- kinetic energy distributions were previously reported for $^{12}_\Lambda$C MWD only [186].

The careful study of the FINUDA π^- kinetic energy spectra permitted an important and careful confirmation of the elementary mechanism that is supposed to underlie the MWD process through the determination of the decay rates. In particular, the ratios $\Gamma_{\pi^-}/\Gamma_\Lambda$ were determined from the measured branching ratios, using available $\Gamma_{\text{total}}/\Gamma_\Lambda$ values or by resorting to a linear fit to the known values for all measured Λ-hypernuclei in the mass range A = 4–12, taken from [187]. The results, reported in figure 4, are in good agreement with previous experimental data, when existing, and with the outcome of some theoretical calculations. This investigation also gave information on the spin-parity (J^π) of the initial hypernucleus ground state thanks to the study of the structure and of the energy dependence of MWD π^- spectra. In this respect, the analysis of MWD can be hence regarded as an indirect spectroscopic investigation tool. This way it was possible to confirm the previous J^π assignment for $^7_\Lambda$Li, $^9_\Lambda$Be, $^{11}_\Lambda$B and to make for the first time the assignment $J^\pi(^{15}_\Lambda N_{g.s.}) = 3/2^+$. Such an achievement demonstrated that the study of MWD product spectra has strong potentialities in the determination of the ground state spin-parity in the case of s- and p-shell hypernuclei; as far as sd-hypernuclei are concerned, also in this case the spectroscopy of particles emitted in the decay process can help in fixing the spectroscopic configuration of the ground state, even though measurements are affected by larger and larger errors, due to the rapid vanishing of the MWD branching ratios. This analysis technique could be then considered
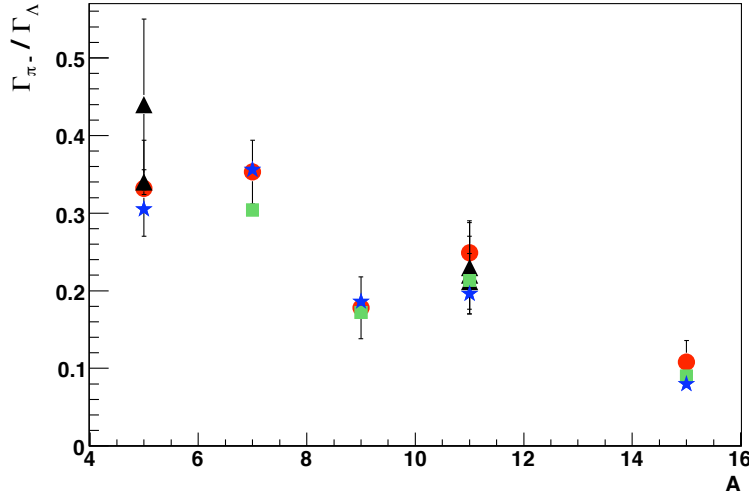
Figure 4. $\Gamma_{\pi^-}/\Gamma_\Lambda$ ratios obtained by the FINUDA experiment (red circles) [181], compared with previous measurements (black triangles) [143, 144, 163, 186, 188] and with theoretical calculations [184, 185] (green squares) and [189] (blue stars) (from [190]).

a complementary spectroscopic tool to the γ-ray spectroscopy of low-lying exited states [10], when the spin ordering cannot be assessed; ultimately it represents a new version of the pioneering technique based on the study of the angular distribution of the MWD π^-, which made possible the determination of the ground state spin-parity for light hypernuclei produced in emulsion and bubble chamber experiments [173–179].

5.3. Non-mesonic weak decay

A full knowledge of the two-nucleon stimulated processes is universally considered a fundamental step in drawing a coherent picture of hypernuclear NMWD. To this purpose many detailed calculations were (and still are) performed in order to predict the contribution of such a channel to the total NMWD width, which is generally believed to be of the order of 20%. A complete list of these theoretical activities can be found in [140]. However, from the experimental point of view, hypernuclear NMWD was scarcely studied up to few years ago essentially because its observation represents a challenging task. First, it is necessary to produce and to identify Λ-hypernuclei in their ground state by means of a performing magnetic spectrometer. Then, all the final state nucleons in (5.2*a*), (5.2*b*) and (5.3*a*), including neutrons, should be detected in coincidence and their energy, along with their angular correlations, should be precisely measured. Moreover, there is an inherent limitation in extracting the physical observables of interest due to the not negligible distortion introduced by FSI on the final state nucleon kinetic energy spectra. Actually, the information about particle initial bare momenta and flight direction may be completely lost; also, their contribution can be mixed and then possible additional quantum-mechanical interference effects can arise [191]. All this makes it challenging to associate to any detected particle its own source, that is to understand which process, one- or two-

induced NMWD or FSI, originated it.

First generation experiments were carried out at BNL [143] and KEK [144]. Afterwards, the SKS Collaboration measured proton and neutron kinetic energy distributions from NMWD of $^5_\Lambda$He and of $^{12}_\Lambda$C, produced via the (π^+, K^+) reaction at 1.05 GeV/c [192]. One of the first attempts to determine the strength of the two-nucleon induced contribution to NMWD width was carried out by fitting the single- and the double-coincidence nucleon energy spectra, measured with good statistics for $^{12}_\Lambda$C, with an Intra-Nuclear Cascade (INC) model suitably tailored for the purpose [193]. The value for the ratio between the two-nucleon induced decay width and the total NMWD one, best reproducing the experimental data, was found to be $\Gamma_{2\mathcal{N}}/\Gamma_{\mathrm{NMWD}} = (0.29 \pm 0.13)$.

A totally different and innovative approach was followed by the FINUDA Collaboration, which recently provided a systematic study of NMWD: in an early paper [194], $^5_\Lambda$He, $^7_\Lambda$Li and $^{12}_\Lambda$C NMWD proton kinetic energy distributions were presented and discussed; afterwards, proton spectra from NMWD of $^9_\Lambda$Be, $^{11}_\Lambda$B, $^{13}_\Lambda$C, $^{15}_\Lambda$N and $^{16}_\Lambda$O were obtained and analyzed [195]. Figure 5 shows all the experimental distributions, background subtracted and acceptance corrected: up to now, they represent a unique database for p-shell Λ-hypernuclei in the A range (5 – 16). The proton kinetic energy spectra are affected by considerable errors, especially in the low energy region, due to the limited statistics. Nevertheless, it was possible to identify some common features: a peak centered around 80 MeV (which corresponds approximately to half of the Q-value for the free $\Lambda p \to np$ reaction) is broadened due to the Fermi motion of nucleons and more and more blurred as A increases; the low energy side of that structure is smeared by a rise that can be ascribed to protons from two-nucleon induced weak decays and from FSI. Finally, thanks to the fit of the high energy region of the spectra (> 80 MeV) to a Gaussian curve, it was possible to identify a clear, increasing trend of the Gaussian mean value as function of A. The original idea, fully described in [195], was then to develop a method in order to disentangle in the proton spectra the contribution due to two-induced NMWD from the ones due to one-induced process and to FSI, without resorting to any INC calculation or constrained fit as it was done instead in [193, 196]. This was actually possible thanks to few very basic assumptions, namely: the number of protons from (5.3a) is less than 5% in the spectrum region beyond 80 MeV, as argued in [191]; the FSI importance depends linearly on A and both $\Gamma_{2\mathcal{N}}/\Gamma_{\mathrm{NMWD}}$ and Γ_n/Γ_p can be considered constant in the A range under study, according to the conclusions reported in [140]. The final results of this model independent analysis were $\Gamma_{2\mathcal{N}}/\Gamma_p = (0.43 \pm 0.25)$ and $\Gamma_{2\mathcal{N}}/\Gamma_{\mathrm{NMWD}} = (0.24 \pm 0.10)$, where the latter determination was obtained by using Γ_n/Γ_p experimental values available in literature [197]. Even more precise determinations were then achieved by taking into account the kinetic energy spectra of pairs of proton and neutron, detected in coincidence. By introducing some further kinematical and topological constraints, the new values turned out to be $\Gamma_{2\mathcal{N}}/\Gamma_p = \left(0.39 \pm 0.16_{\mathrm{stat}}\,^{+0.04}_{-0.03}\,_{\mathrm{syst}}\right)$ and $\Gamma_{2\mathcal{N}}/\Gamma_{\mathrm{NMWD}} = \left(0.21 \pm 0.07_{\mathrm{stat}}\,^{+0.03}_{-0.02}\,_{\mathrm{syst}}\right)$ [198], obtained by exploiting again the measured Γ_n/Γ_p values [197]. Such a FINUDA result substantiated the most recent theoretical prediction for $\Gamma_{2\mathcal{N}}/\Gamma_{\mathrm{NMWD}} = 0.26$ [199]. Finally, the outlined analysis provided as well the first experimental evidence for the process (5.3a): three candidate events were extracted from the available data sample. A complete kinematical reconstruction of the three-nucleon final state identified two $^7_\Lambda$Li $\to$ ^{4}He + n + n + p events and one $^9_\Lambda$Be $\to$ ^{3}He + ^{3}H + n + n + p decay [190].
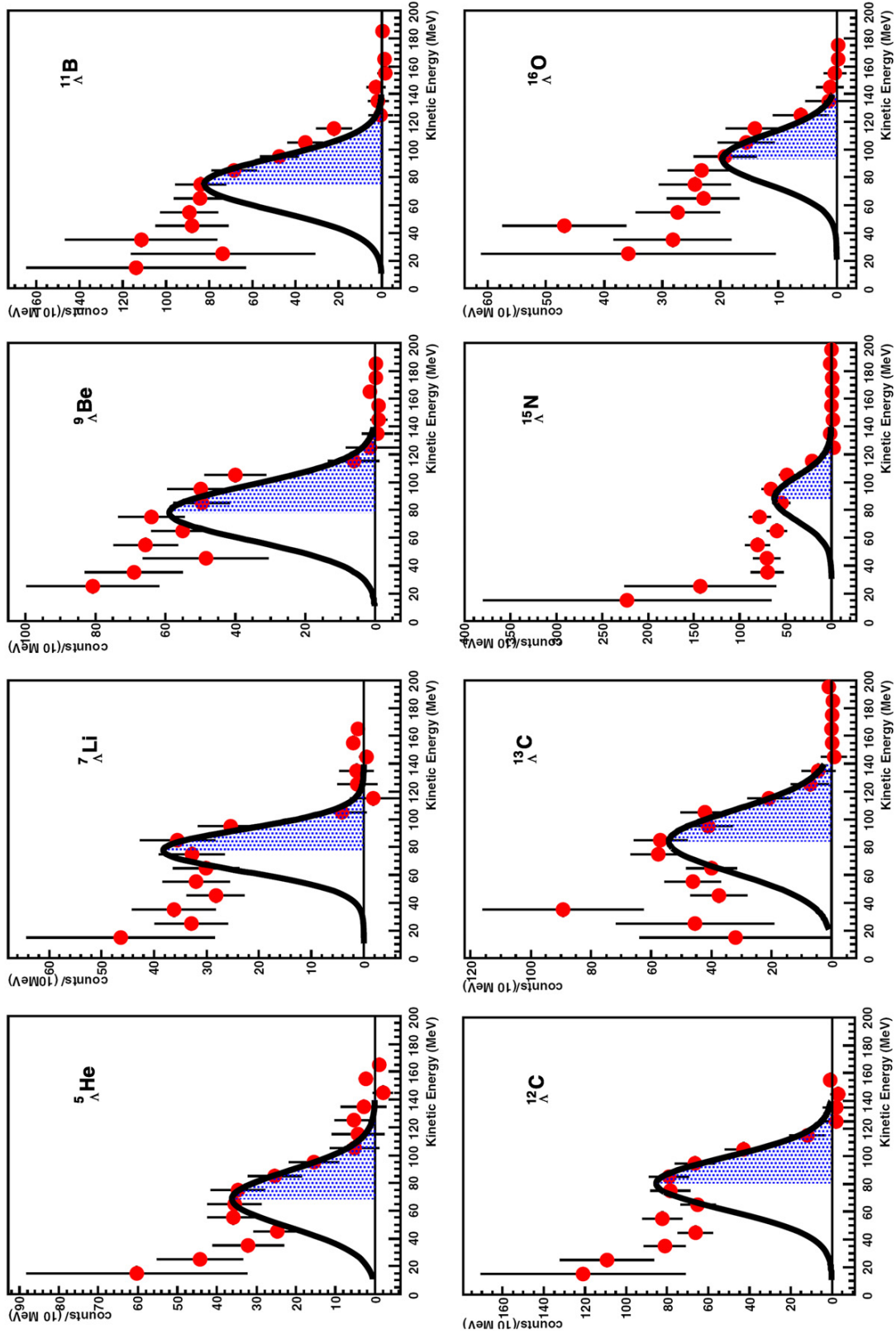
Figure 5. Proton kinetic energy spectra from the NMWD of (from right to left, top to bottom): $^{5}_{\Lambda}$He, $^{7}_{\Lambda}$Li, $^{9}_{\Lambda}$Be, $^{11}_{\Lambda}$B, $^{12}_{\Lambda}$C, $^{13}_{\Lambda}$C, $^{15}_{\Lambda}$N and $^{16}_{\Lambda}$O. The blue hatched area indicates the region of the spectrum where the two-nucleon induced NMWD contribution could be considered negligible (from [195]).

6. Other strange nuclear systems

In the case of Λ-hypernuclei, the decay mode from the ground state is a weak process which proceeds through either the mesonic $\Lambda \to \pi^- p / \pi^0 n$ or the non-mesonic $\Lambda \mathcal{N} \to \mathcal{N} \mathcal{N}$ and $\Lambda \mathcal{N} \mathcal{N} \to n \mathcal{N} \mathcal{N}$ channels, as discussed in Section 5. When heavier hyperons such as Σ or Ξ are bound in a nucleus, the situation is drastically different from Λ-hypernuclei. They are no longer stable against strong decays even in their ground states. Therefore, Σ- and Ξ-hypernuclei are quasi-bound systems, provided that they exist. Both of them undergo to the strong decay conversion process $\Sigma \mathcal{N} \to \Lambda \mathcal{N}$ and $\Xi \mathcal{N} \to \Lambda \Lambda$, respectively. These conversion processes introduce spreading widths for the quasi-bound states, which makes experimental identifications of the bound states non-trivial.

6.1. Σ-hypernuclei

Studies of Σ-hypernuclei gave us a good example on how to extract the Σ-nucleus optical potential information through the X-ray measurements of Σ^- atoms. Due to strange quark inside, strange particles have negatively charged states: Σ^-, Ξ^-, K^-. When these negative particles are stopped inside a material, they happen to form exotic atoms like Σ^--, Ξ^-- and K^--atom. These atoms de-excite by emitting X-rays and the strange particles are finally absorbed by the nucleus. The last X-ray emitted before the absorption eventually has information about the energy shift and finite width due to the Σ^--nucleus strong interaction. The energy shift corresponds to the real part of the Σ^--nucleus potential, $\Re(V_{opt.}^{\Sigma \mathcal{N}}(r))$, while the width to the imaginary part, $\Im(V_{opt.}^{\Sigma \mathcal{N}}(r))$.

Here, it should be noted that the sensitive fraction of the distance from the nuclear center r is near the surface of a nucleus, where the nuclear density is very low. Therefore, an extrapolation to the nuclear center, $V_{opt.}^{\Sigma \mathcal{N}}(r), r \to 0$, at normal nuclear density ρ_0 is required. Since this extrapolation is model-dependent, the estimation of the existence of a bound state usually has a large uncertainty.

Anyway, using the energy shifts and widths of the Σ^--atom X-rays the real and imaginary parts of the optical potential $V_{opt.}^{\Sigma N}(0)$ were estimated to be 25-30 MeV and 10-15 MeV respectively, based on the $t\rho$ type potential [200, 201]. The width of a bound state is estimated to be $\sim -2\mathrm{Im}V_{opt.}^{\Sigma \mathcal{N}}(0)$. Therefore, it would be too large (20-30 MeV) to be experimentally observed as a clear peak.

Thus, it was a big surprise that the Heidelberg-Saclay-Strasbourg Group reported two narrow structures in the unbound region of the $^9\mathrm{Be}(K^-, \pi^-)$ spectrum in 1980 [202]. From the similarity of such a spectrum with the $^9_\Lambda \mathrm{Be}$ one, they claimed that there were two narrow peaks with a width less than 8 MeV. Thereafter, the narrow width of Σ-hypernuclei had been an important issue in the 80's both theoretically and experimentally. The situation at that time is well summarized in [203].

Several other narrow structures were observed at CERN, BNL, and KEK in $^6\mathrm{Li}(K^-, \pi^\pm)$, $^7\mathrm{Li}(K^-, \pi^-)$, $^9\mathrm{Be}(K^-, \pi^+)$, $^{12}\mathrm{C}(K^-, \pi^\pm)$ and $^{16}\mathrm{O}(K^-, \pi^\pm)$ reactions, all in the unbound region but with a poor statistical significance.

For the most statistically significant peaks reported in the $^9\mathrm{Be}(K^-, \pi^\mp)$ reaction, almost a ten-times larger data sample was collected in BNL-AGS E887 experiment in 1994, by using the Moby-Dick spectrometer [204]. No narrow states were observed above the binding threshold; the study of the $^6\mathrm{Li}(K^-, \pi^-)$ reaction [205] provided a negative result as well. Thus, the existence of narrow Σ-hypernuclear states above the
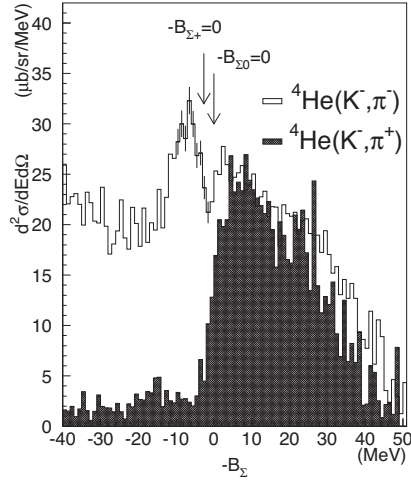
Figure 6. Excitation energy spectra of $^4\text{He}(K^-, \pi^-)$ and $^4\text{He}(K^-, \pi^+)$ at 600 MeV/c K^- momentum, measured at 4° (from [212]).

binding threshold was excluded experimentally, even though none of the experimental spectra was sensitive in the bound region of Σ, including the BNL E887 data.

On the other hand, in theoretical analyses on Σ^--atom X-rays, Σ-nucleus potentials taking into account the density dependence were introduced, motivated by the newly published precise X-ray data on W and Pb targets [206]. Apparently, there was a significant improvement in the fitting outcome and its result suggested that the real part of the potential was strongly repulsive inside heavy nuclei [207–209]. This was a surprise for experimentalists. Then, whether Σ-nucleus bound states exist or not became an issue.

At that time there was one experimental report claiming evidence for a bound state $^4_\Sigma\text{He}$ observed in the $^4\text{He}(K^-_{\text{stop}}, \pi^-)$ reaction in 1989 [210]. However, there were some difficulties in extracting reliably its binding energy and its width both experimentally and theoretically from this reaction. From the experimental side, the $(K^-_{\text{stop}}, \pi^-)$ reaction has several concurrent processes generating a large background just under the bump signal [211]. From the theoretical point of view, the ambiguity on the initial wave function of atomic K^- orbits from which the kaon is absorbed produces different spectrum shapes in theoretical calculations. Because of these ambiguities, there was no conclusion whether the observed bump structure was an unstable bound state or a threshold cusp.

A definite answer was obtained in the BNL E905 experiment [212]. The $^4\text{He}(K^-, \pi^\mp)$ spectra were measured at 600 MeV/c K^- incident momentum. In the in-flight reaction, the interaction mechanism is simple and theoretical analyses are more reliable. Further, the physical pion backgrounds from the hyperon decays are out of the apparatus acceptance in momentum. A clear peak below the Σ binding threshold was observed in the $^4\text{He}(K^-, \pi^-)$ spectrum (see figure 6). No peak was observed in the $^4\text{He}(K^-, \pi^+)$ spectrum. The obtained binding energy was $(4.4 \pm 0.3_{\text{stat}} \pm 1_{\text{syst}})$ MeV and the width (FWHM) was $(7.0 \pm 0.7_{\text{stat}} {}^{+1.2}_{-0.0}{}_{\text{syst}})$ MeV. The

analysis suggests that the $^4_\Sigma$He bound state has isospin $T = 1/2$. The existence of such a $T = 1/2$ and $S = 0$ bound state in $^4_\Sigma$He was first predicted by Harada *et al.* [213]. It has unique nature of large isospin dependence: $T = 1/2$ state is attractive, while $T = 3/2$ state is strongly repulsive. In the attractive $T = 1/2$ channel there exists a central repulsion in the Σ-nucleus potential which decreases the $\Sigma\mathcal{N} \to \Lambda\mathcal{N}$ conversion width by reducing the overlap of the Σ wave function with a nuclear core.

Through an analysis using the E905 data, Harada obtained the complex pole position at $(-1.1 - i6.2)$ MeV [214]. Thus, the existence of a Σ hypernuclear bound state was established. However, it suggested that the central iso-scalar part of the Σ-nucleus potential was indeed repulsive so that, when heavier isospin-saturated systems are considered, there would be no bound states.

The repulsive nature of the Σ-nucleus potentials in medium to heavy systems was experimentally demonstrated in KEK-PS E438 for the (π^-, K^+) reaction on CH_2, Si, Ni, In and Bi targets at 1.2 GeV/c [215–217]. Qualitatively, the spectrum near the Σ^- binding threshold is enhanced when the real part of the potential is attractive, while the shape is suppressed, or moved away into the higher excitation region, when it is repulsive. By using Woods-Saxon type potentials, the obtained (π^-, K^+) spectra were well reproduced with about 90 MeV for the real part and -40 MeV for the imaginary part [217].

Harada and Hirabayashi [218] carried out calculations to reproduce the ^{28}Si(π^-, K^+) spectrum by using various types of potential forms including the density-dependent one. They found that fully attractive potentials failed to fit the data, while repulsive ones with 10–40 MeV strength fit the data very well.

In conclusion, it is a present consensus that there would be no bound Σ-hypernuclear systems in medium to heavy systems; there could be a few more in light systems owing to the spin-isospin dependence of the Σ-nucleus potentials.

6.2. S = −2 hypernuclei

Experimental information for $S = -2$ systems are very much limited, because high-intensity medium energy K^- beams are required to produce such objects. In the $S = -2$ systems, we have Ξ- and double Λ-hypernuclei. In the former case, the $S = -2$ is contained in one baryon Ξ, while it is separately shared by two $S = -1$ Λs in the latter case. The existence of double Λ-hypernuclei is already established by several emulsion events; $_{\Lambda\Lambda}^6$He was cleanly identified in the "Nagara" event [219], in particular. Clear experimental identification of Ξ-hypernuclei has not yet been successful, although there are several candidate emulsion events and evidence was claimed in a (K^-, K^+) excitation energy spectrum [220].

These systems are coupled through the $\Xi p \to \Lambda\Lambda$ conversion process with strong interaction; the coupling strength is also not well known. The Q value of the conversion reaction in free space is only 28.3 MeV as shown in figure 7. There could be some mixing effects between the two systems. The best way to implant a double strangeness content into a nucleus with clean experimental identification is to start from the two-body reaction $K^- p \to K^+ \Xi^-$. The K^- incident momentum dependence of the production cross section shows a broad maximum at around 1.8 GeV/c [222]. In this momentum region, it is not trivial to obtain a high-intensity K^- beam with a good purity. Nevertheless, a good K^- to π^- ratio better than 1 was achieved at the BNL D6 beam line [58] by installing a double-stage electro-static separator system. The angular distribution of the cross section was also measured and found to be not
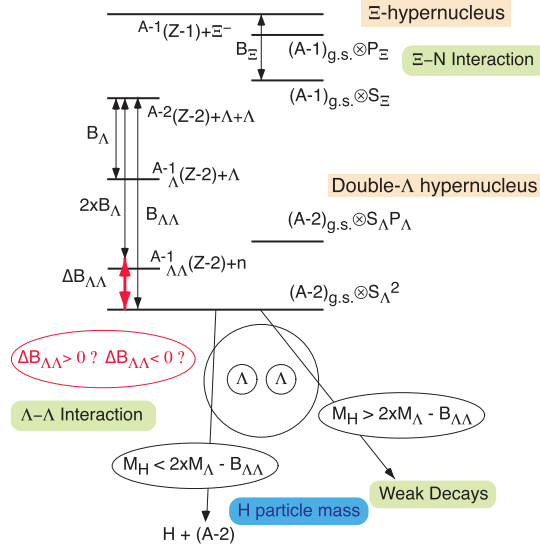
Figure 7. Typical energy spectrum and decay thresholds for $S = -2$ systems; Ξ and double Λ hypernuclear configurations (see [221]).

sharply peaked in the forward direction. However, it is still effective to produce Ξ^-s in the forward direction in the Laboratory system due to the Lorentz boost.

Starting from the production of Ξ^- via the $K^-p \to K^+\Xi^-$ reaction, so far, three processes have been experimentally utilized to implant $S = -2$ (see figure 8).

One method is to stop the produced Ξ^- in a secondary target after degrading the Ξ^- energy inside the primary target material. Since the recoil momentum of the Ξ^- in the production stage is around 500 MeV/c, there is a competition between the stopping time and the Ξ^- life time ($\beta\gamma c\tau_{\Xi^-} \approx 1.86$ cm) and most of the Ξ^-s tend to decay before stopping. Once they stop, a Ξ^- atom is formed. A Ξ^- cascades down the atomic orbits by emitting X-rays. At some inner atomic orbit, the Ξ^- is absorbed by a nucleus via the $\Xi^-p \to \Lambda\Lambda$ conversion. The probability of this absorption per quasi-free Ξ^- is of the order of 0.1% which is limited mainly by the low stopping efficiency. After the absorption, a highly-excited continuum state with two Λs, which is usually indicated as "Double Λ Compound States" [224], is formed. This state normally de-excites by emitting a few nucleons and one or two Λs. It occasionally emits a double Λ-hyperfragment or two Λ-hyperfragments in the final state. This method has been applied in hybrid-emulsion experiments to produce double Λ-hypernuclei, which are identified through sequential weak decay patterns in emulsion.

The effectiveness of the second method was first demonstrated in BNL E906 experiment [225]. The method uses the production nucleus as an energy degrader for the Ξ^- at the same time. Since the recoil momentum of the Ξ^- is high, several $\Xi^-\mathcal{N} \to \Xi^-\mathcal{N}$ collisions in the nucleus would be necessary to slow down the Ξ^- and eventually it would be absorbed via the $\Xi^-p \to \Lambda\Lambda$ process. This situation is similar to the "Double Λ Compound States" formed after the Ξ^--atom absorption process. Considering a typical mean free path of a Ξ^-, the formation of the "Double Λ

Compound States" through direct quasi free process would be comparable ($\sim 0.3\%$) to the first method for $A = 9 - 12$ target nuclei. Another source of the "Double
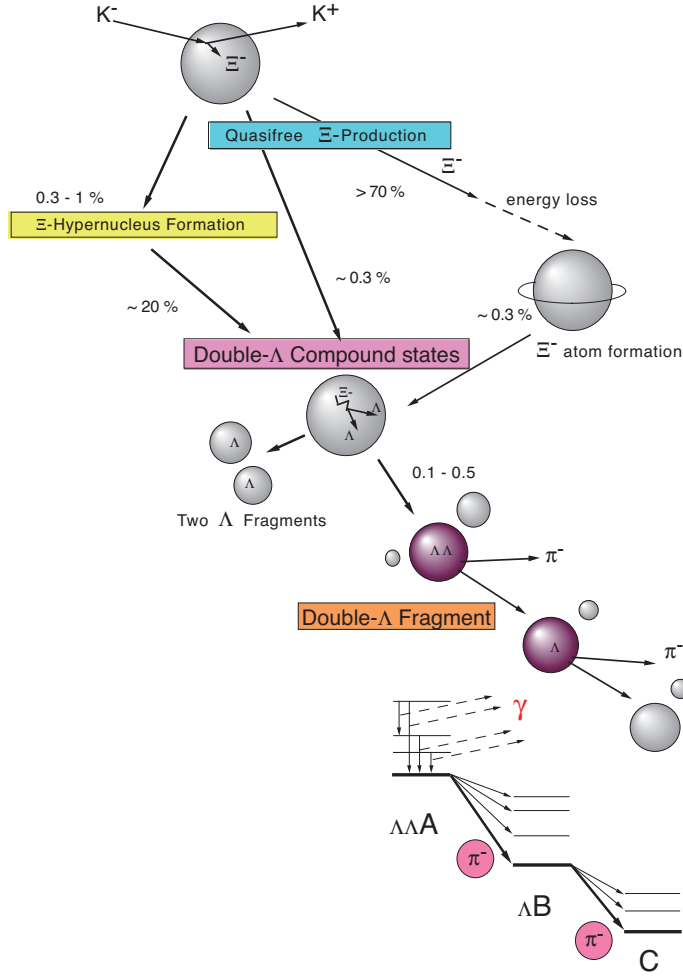

Figure 8. Reaction processes to produce Ξ- and double Λ-hypernuclei in the (K^-, K^+) reaction (from [223]).

Λ Compound States" formation was suggested through the direct Ξ-hypernuclear formation. If Ξ-hypernuclear bound states exist, we can produce them with the (K^-, K^+) reaction directly. Since the Ξ^- recoil momentum is high, the sticking probability of the Ξ^- would not be so large (0.3–1%). However the Ξ-hypernuclei should be converted to the "Double Λ Compound States" with high probability because the Ξ^- is already bound in the nucleus. This process would also have a formation probability of the order of 0.1%.

The direct population of double Λ-hypernuclei in the (K^-, K^+) reaction has been discussed theoretically. Simple two-step calculations such as $K^-p \rightarrow \pi^0\Lambda$, $\pi^0 n \rightarrow K^+\Lambda$ give us very small production cross sections of the order of nb/sr. Enhancements are expected through the $\Xi^-p \rightarrow \Lambda\Lambda$ coupling.

A series of hybrid-emulsion experiments at KEK-PS, E176 [226] and E373 [227], have been very much successful in establishing the existence of double Λ-hypernuclei and in determining the binding energy of $_{\Lambda\Lambda}^{6}$He. Before these observations, there were a few old emulsion events. However, the identification and the interpretation of these events was criticized at that time. A new event observed in E176 had established the existence of double Λ-hypernuclei by cleanly identifying the sequential weak decay pattern. In order to have an unambiguous identification of double Λ hypernuclear species it was necessary to wait for the E373 experiment result. In the "Nagara" event, $_{\Lambda\Lambda}^{6}$He was uniquely identified and its binding energy was measured. The $\Lambda - \Lambda$ binding energy ($\Delta B_{\Lambda\Lambda} \equiv B_{\Lambda\Lambda} - 2B_{\Lambda}$) was obtained to be (0.67 ± 0.17) MeV [227]. This value of $\Delta B_{\Lambda\Lambda}$ is smaller than the previously estimated value by $\sim$4.7 MeV.

There is almost no experimental information on two-body $\Xi\mathcal{N}$ interaction. Very limited information is available for elementary processes. One measurement [228] used a scintillation fiber detector as an active target to measure the $\Xi p \to \Xi p$ and $\Xi^{-}p \to \Lambda\Lambda$ reactions in the Ξ^{-} momentum range of 0.2 GeV/c to 0.8 GeV/c. They observed one candidate for the $\Xi^{-}p$ elastic scattering and three for the $\Xi^{-}p \to \Lambda\Lambda$ in ^{12}C. From this analysis, an upper limit for the elastic cross section was obtained to be 24 mb at 90% confidence level, and $4.3^{+6.3}_{-2.7\text{stat}}$ mb for the latter inelastic channel. The other measurement [229] observed the $\Xi^{-}\mathcal{N}$ scattering in ^{9}Be, and obtained the elastic scattering cross section for an average Ξ^{-} momentum of 550 MeV/c to be $\left(30.7 \pm 6.7_{\text{stat}} {}^{+3.7}_{-3.6\,\text{syst}}\right)$ mb.

Therefore, it is useful to extract the strength of the real part of the Ξ-nucleus potential from shape analyses on the (K^{-}, K^{+}) reaction near the binding threshold region, as was carried out for the Σ-nucleus potential. Unfortunately, there have been no dedicated measurements on the (K^{-}, K^{+}) missing-mass spectra with good energy resolution. In KEK-PS E224 [230], the ^{12}C(K^{-}, K^{+}) spectrum at 1.6 GeV/c was obtained with an energy resolution of 9.5 MeV in σ. On the basis of the shape analysis near the Ξ binding threshold, it was claimed the potential depth V_0^{Ξ} was shallower than 20 MeV. Later, in the BNL E885 experiment [220], the ^{12}C(K^{-}, K^{+}) spectrum at 1.8 GeV/c was obtained with 10 times better statistics and better energy resolution of 6.1 MeV in σ. In fact, they observed a significant number of events (about 40–60) in the bound region and they claimed the evidence of Ξ-hypernuclear bound state production. They reported a cross section value for the ^{12}C$(K^{-}, K^{+})^{12}_{\Xi}$Be reaction of (89 ± 14) nb/sr $((42 \pm 5)$ nb/sr) for the angular average from 0° to 8° (0° to 14°). The Ξ-nucleus potential well depth V_0^{Ξ} was preferred to be about 14 MeV within the Woods-Saxon prescription.

7. Antimatter Λ-hypernuclei

Very often hypernuclear physics is mentioned because it added a third dimension to the traditional Z-N nuclear chart, by taking into account the strangeness flavor quantum number S. Very recently this 3D picture, that classifies bound nuclear systems on the basis of their net strangeness content (S = 0, -1, -2, ...), has been extended to the region characterized by both Z and N negative values and positive strangeness S, that is in the antimatter sector.

The STAR experiment, installed on the BNL RHIC, has the merit of having observed for the first time the $^{3}_{\bar{\Lambda}}\overline{\text{H}}$, that is a bound system made of an $\bar{p}$, an $\bar{n}$ and an $\bar{\Lambda}$, in Au + Au collisions at $\sqrt{s_{NN}} = 200$ GeV [170, 231, 232]. The data analysis procedure to extract the $^{3}_{\bar{\Lambda}}\overline{\text{H}}$ (and $^{3}_{\Lambda}$H) signal was very challenging and such a discovery

must be considered as having found a needle in a haystack. It confirmed that every physical system has an antimatter partner of the same mass in a new context, the one of Λ-hypernuclei. Moreover the study of hypertritium and antihypertritium offers the opportunity to investigate the dynamics of ultrarelativistic heavy-ion collisions.

The $^{3}_{\Lambda}\overline{\text{H}}$ production has been subsequently confirmed by the ALICE experiment, running at the CERN LHC, in Pb + Pb collisions at $\sqrt{s_{NN}} = 2.76$ TeV [233].

In both cases the key tool for $^{3}_{\Lambda}\text{H}$ and $^{3}_{\Lambda}\overline{\text{H}}$ observation was the detection of charged decay products, following hypertriton and antihypertriton mesonic weak decay (see subsection 5.2):

$$^{3}_{\Lambda}\text{H} \rightarrow {}^{3}\text{He} + \pi^{-}, \tag{7.1}$$

$$^{3}_{\Lambda}\overline{\text{H}} \rightarrow {}^{3}\overline{\text{He}} + \pi^{+}. \tag{7.2}$$

The identification of the final state charged particles has been made possible by the excellent performance of both the STAR and the ALICE apparatuses in terms of particle identification, based on the information provided by their Time Projection Chamber (TPC). The STAR experiment best-fit value for the antihypertriton mass turned out to be $m\left(^{3}_{\Lambda}\overline{\text{H}}\right) = (2.991 \pm 0.001_{\text{stat}} \pm 0.002_{\text{syst}})$ GeV/c^2, to be compared with the ALICE determination $m\left(^{3}_{\Lambda}\overline{\text{H}}\right) = (2.993 \pm 0.001)$ GeV/c^2. As far as the width of the isolated signal is concerned, a value of $\sigma = 2.5 \times 10^{-3}$ GeV/c^2 and of $\sigma = (2.00 \pm 1.20) \times 10^{-3}$ GeV/c^2 is reported by the STAR and the ALICE Collaborations, respectively.

8. Deeply bound $\overline{K}$-nucleus states

8.1. Overview

The study of kaonic nuclei is going to open a new paradigm of hadronic many-body system with strangeness. While hypernuclei, so far investigated, are nuclear systems with strangeness composed of only baryons, the kaonic nuclei are the new type of hadronic many-body system composed of meson and baryons.

A main driving force to make the kaonic nuclei to exist is the strong attraction of $\overline{K}\mathcal{N}$ interaction in isospin $I = 0$ channel. Such information on the $\overline{K}\mathcal{N}$ interaction near threshold has been obtained by analyzing K^{-}-atom X-ray data, low-energy $K^{-}p$ scattering data and measurements of several threshold branching ratios. The recent high-precision kaonic hydrogen X-ray measurement by the SIDDHARTA collaboration [234, 235] has a significant contribution in constraining theoretical models. Nevertheless, there still exist discussions on how strong the attraction is: deep ($\Re(V_{\overline{K}})=-(150\text{-}200)$ MeV) or shallow ($\Re(V_{\overline{K}})=-(40\text{-}60)$ MeV). There have been a lot of theoretical works on this subject. Since it is beyond the scope of the present review, here we refer to a few recent articles [236–238].

8.2. Critical review of experimental results

In this subsection, several experimental results are reported. The situation is not conclusive for the existence of kaonic nuclei, yet. Some groups reported a signal, but some did not. In general, it looks hard to observe the signal in inclusive missing-mass spectra. It means that the production rate of kaonic nuclei would be not so large compared with standard strangeness production processes and the signal could be hidden under such large backgrounds.

Some coincidence measurements with the decay products from kaonic nuclei would be needed to suppress the background. In this respect, invariant-mass measurements in a specific decay mode, such as Λp, Λd, and Λt pairs [239], were carried out by several groups. Among them, the experimental focus has been intensively put on the $K^- pp$ system decaying into Λ and proton, because it would be the simplest kaonic nuclei, provided that they exist.

The first experimental evidence for the $K^- pp$ bound state was reported by the FINUDA experiment at DAΦNE [240]. In the stopped K^- absorption reaction on ^{6}Li, ^{7}Li, and ^{12}C, a large number of Λp pairs, back-to-back emitted, were observed. If the mass of the emitted object was close to the mass of a K^- plus two protons, this process would be nothing but non-mesonic two-nucleon absorption of $K^- + pp \to \Lambda p$ by two-proton pair. However, the invariant mass distribution of the $\Lambda - p$ pairs showed a significant mass shift to the lighter mass side (see figure 9). It was interpreted as a signal of the $K^- pp$ bound state formation decaying into Λ and proton with a large binding energy. A binding energy of $\left(115^{+6}_{-5\,\text{stat}}\,{}^{+3}_{-4\,\text{syst}}\right)$ MeV and a width of $\left(67^{+14}_{-11\,\text{stat}}\,{}^{+2}_{-3\,\text{syst}}\right)$ MeV were obtained.
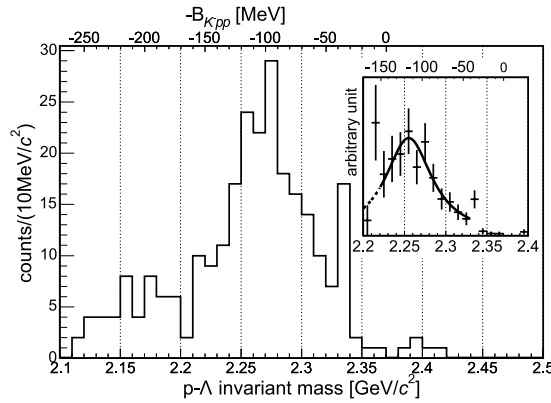

Figure 9. Invariant mass of a Λa and a proton in back-to-back correlation $(\cos\theta^{Lab} \leq -0.8)$ from the stopped K^- reactions on ^{6}Li, ^{7}Li, and ^{12}C targets in the FINUDA experiment. The inset shows the result after the acceptance correction (from [240]).

The reaction mechanism to produce such a deeply-bound $K^- pp$ system in the stopped K^- absorption is not known well. The interpretation by FINUDA was criticized by taking account of the final state interactions after the quasi-free two-nucleon absorption process [241]. While this effect shifts the invariant mass in to the low-mass side as observed, the back-to-back correlation would be lost at the same time.

The missing-mass measurement was carried out for the $^4\text{He}(K^-_{\text{stop}}, p)$ [242] and $^4\text{He}(K^-_{\text{stop}}, n\pi^\pm)$ [243] reactions in KEK-PS E549 experiment to look for $K^- pnn/K^- ppn$ systems. In these high-statistic inclusive spectra, no narrow structures ≤ 40 MeV/c^2 were observed. In the case of $K^- pnn$, the upper limits of the formation branching ratio with an assumed width of 0, 20, 40 MeV/c^2 were determined to be $(0.4$–$6)\times10^{-4}$, $(0.2$–$6)\times10^{-3}$ and $(0.06$–$5)\times10^{-2}$/(stopped K^-), respectively, with 95% confidence level, in the mass range $3000 < M < 3200$ MeV/c^2. In the case of $K^- ppn$, the upper limits at 95% confidence level with the width of 0 and 20 MeV/c^2

were at most 1%.

The OBELIX Group analyzed their data of $\bar{p}^4$He annihilations at rest [244, 245]. In the invariant mass of the $p\pi^- - p$ coming from Λp, a narrow peak with a width $< (33.9 \pm 6.2)$ MeV was observed with the binding energy of $(-151.0 \pm 3.2_{\text{ stat}} \pm 1.2_{\text{ syst}})$ MeV for $K^- pp$ (or $_{\bar{K}}^2$H) with a statistical significance of 4.7σ. There were some difficulties to clearly identify the Λ and the peak width measurement was limited due to the detector resolution.

In the DISTO experiment at the SATURNE accelerator at Saclay, the exclusive reactions of $pp \to p\Lambda K^+$ at 2.85 GeV and 2.50 GeV were investigated to search for the $K^- pp$ [246, 247]. Both missing-mass and invariant-mass distributions were obtained. A broad enhancement was found at 2.85 GeV by selecting the emission angles of K^+ and p, while a very small cross section was observed at 2.50 GeV. From the observation, a binding energy of $(103 \pm 3_{\text{ stat}} \pm 5_{\text{ syst}})$ MeV and a width of $(118 \pm 8_{\text{ stat}} \pm 10_{\text{ syst}})$ MeV were obtained.

In-flight $(K^-, n/p)$ reactions at the K^- incident momentum of 1 GeV/c were used to produce kaonic nuclei in KEK-PS E548 experiment [248]. The inclusive spectra of the ^{12}C(K^-, n) and ^{12}C(K^-, p) reactions were measured. While they observed a significant number of events in the K^- bound region, they were not able to observe any clear peak structures corresponding to bound states. From the spectrum shape analysis, they estimated the K^- potential depths of -190 MeV and -160 MeV for ^{12}C(K^-, n) and ^{12}C(K^-, p), respectively, which suggests that the $\overline{K}$ nucleus potential is deep.

At LEPS/SPring-8 facility, the $K^- pp$ bound state was searched for in the $\gamma d \to K^+ \pi^- X$ reaction at $E_\gamma = 1.5$–2.4 GeV [249]. The inclusive $K^+ \pi^-$ photo-production off deuterium was measured for the first time in this energy range. There was no peak in the mass region of 2.22 to 2.36 GeV/c^2.

During the phase of the final editing of this review article, the J-PARC E27 experiment has reported the observation of a "$K^- pp$"-like structure in the $d(\pi^+, K^+)$ reaction [250]. The experiment was carried out at the K1.8 beam line in the hadron experimental hall of J-PARC by using the π^+ beam at 1.69 GeV/c. In this reaction, $\Lambda(1405)$ would be produced as a doorway to the $K^- pp$ formation [251]. However, large backgrounds due to hyperon and hyperon resonance production processes affect the inclusive (π^+, K^+) missing-mass measurement. In order to suppress such backgrounds, two-proton coincidence was requested in a range counter array system surrounding the deuterium target. A broad bump structure in the $K^- pp$ mass distribution around 2.27 GeV/c^2 was observed in the $\Sigma^0 p$ decay mode, which corresponds to a $K^- pp$ binding energy of $\left(95_{-17 \text{ stat}}^{+18} {}_{-21 \text{ syst}}^{+30}\right)$ MeV and to a width of $\left(162_{-45 \text{ stat}}^{+87} {}_{-78 \text{ syst}}^{+66}\right)$ MeV.

9. Future perspectives

9.1. Strangeness nuclear physics at J-PARC

At the J-PARC hadron experimental hall, two experiments are scheduled to run in 2015 at this moment. One experiment is E15 to search for the $K^- pp$ bound state in the ^{3}He(K^-, n) reaction at 1 GeV/c. In this experiment, the $K^- pp$ signals will be obtained not only in the missing mass of the (K^-, n) spectrum but also in the invariant mass of the Λ-p pairs from the non-mesonic decay of the $K^- pp$. A large neutron detector system in the forward direction and a cylindrical detector system surrounding the

liquid ^{3}He target are installed in the K1.8BR area. The other experiment is E13 to measure hypernuclear γ-rays with Hyperball-J detector system [16]. The γ-ray transitions of $^4_\Lambda$He($1^+ \to 0^+$) and several new ones in $^{19}_\Lambda$F will be measured. The $\Lambda\mathcal{N}$ spin-spin interaction will be studied in an sd-shell hypernucleus for the first time.

A new hybrid-emulsion experiment E07, "Systematic Study of Double Strangeness System with an Emulsion-Counter Hybrid Method" is in preparation at the K1.8 beam line. They aim to stop about 10 times more Ξ^-s ($\sim 10^3$ Ξ^-s) in emulsion compared with the previous E373 experiment. The KURAMA spectrometer system will be used for the forward K^+ detection. In order to speed up the emulsion analysis, a high-speed automatic scanning system has been developed. By replacing the emulsion system with the Ge detector system, Hyperball-J, an experiment E03 to measure the X-rays from Ξ^--atom can be carried out at the same beam line.

As for the Ξ-hypernuclei, the E05 experiment "Spectroscopic Study of Ξ-Hypernucleus, $^{12}_\Xi$Be, via the ^{12}C(K^-, K^+) Reaction" is constructing a new high-resolution spectrometer S-$2S$ (see figure 10) for the ^{12}C(K^-, K^+)$^{12}_\Xi$Be reaction. The spectrometer is composed of three magnets QQD with a momentum resolution of 5×10^{-4} (FWHM) and a solid angle acceptance of 60 msr. With a goal of the excitation energy resolution of better than 1.5 MeV, the experiment aims to observe the $^{12}_\Xi$Be bound state as a clear peak. The peak position and the width will give us the binding energy and the $\Xi^- p \to \Lambda\Lambda$ conversion strength. Once the existence of Ξ-hypernucleus is established for $^{12}_\Xi$Be, it will be important to observe several light Ξ-hypernuclei in order to investigate spin and isospin dependence of Ξ-nucleus potential. For example, it is discussed that the structures of $^7_\Xi$H and $^{10}_\Xi$Li are important to extract spin- and isospin-averaged Ξ-nucleus potential. These Ξ-hypernuclei can be produced in the ^{7}Li(K^-, K^+) and ^{10}B(K^-, K^+) reactions. There is also a discussion that Coulomb-assisted bound states could be formed in heavy Ξ hypernuclei.
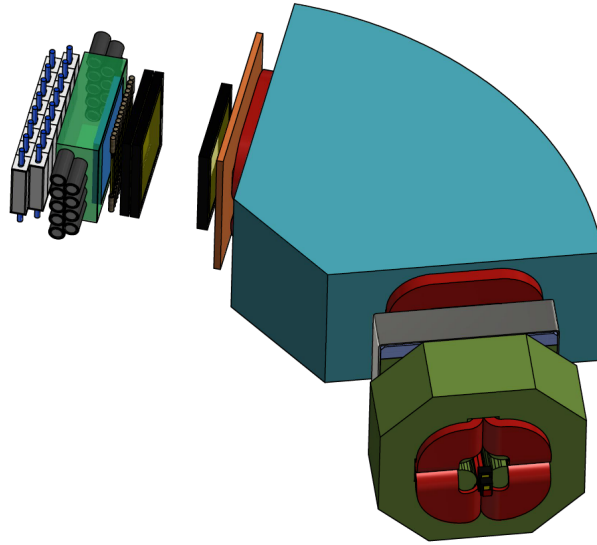

Figure 10. Schematic view of the S-$2S$ spectrometer for the (K^-, K^+) reaction. It consists of three magnets QQD (two quadrupole magnets and one dipole magnet).

9.2. Hypernuclear physics program at JLab

As soon as the ongoing plan of upgrade in energy of the e^- accelerator complex will be completed, JLab is expected to deliver a good wealth of high precision data on structure of a large variety of Λ-hypernuclei, thus offering a unique opportunity for new findings and discoveries.

One of the main topic on which attention will focused is the CSB in the A = 4 hypernuclear iso-doublet. A new measurement of the $^4_\Lambda$H 0^+ and 1^+ energy levels is planned by using the ^{4}He$(e, e'K^+)^4_\Lambda$H reaction. By exploiting the decay pion spectroscopy method, the $^4_\Lambda$H ground state energy is expected to be measured with an accuracy of the order of 10 keV. This activity will be carried out in a synergistic way with the J-PARC E13 experiment which, as mentioned in subsection 9.1, will determine the $^4_\Lambda$He excitation energy with a few keV energy resolution.

Another interesting subject that will be addressed is the investigation of Λ-hypernuclei in the medium to high A range, a program already partially carried out by the E05-115 experiment (see subsection 3.3). Actually, such studies are not just an extension of what has been done in low A region, the kind of information achievable being expected to be completely different. Essentially, all nuclear models agree that the structure of heavy nuclei is dominated by mean-field dynamics. However, measurements on normal nuclei dedicated to test the single particle nature of a nucleon are limited to states near the Fermi surface. Then, it is practically impossible to study the deep inside of nuclear structure through spectroscopy, since Pauli principle prevents the use of a nucleon as a penetrating probe. As already mentioned, the situation is totally different for Λ-hypernuclei: the Λ particle is not affected by the Pauli exclusion principle and then it can freely explore the deep nuclear interior and it can occupy all the allowed energetic levels. The study of heavy Λ-hypernuclei can provide information about several subjects, like the depth of the $\Lambda\mathcal{N}$ potential in the nucleon mean-field, the magnitude of the spin-orbit splitting and the possible core polarization. The final goal is to try to answer the ultimate question, if a nucleon, or more in general a baryon, can exist as a single particle even deep inside of a nucleus or it should be described within a quark picture. From the experimental point of view, high energy resolution of $(e, e'K^+)$ hypernuclear spectroscopy represents an attractive tool to perform a systematic survey of medium/heavy Λ-hypernuclei, even though one should keep in mind the issue of the severe background due to bremsstrahlung and Møller scattering in high Z targets. Also in this case, the result of these investigations can have important reverberations on the understanding of the neutron star composition, as far as the presence of strange matter is concerned.

Finally, it was recently proposed to use magnetic spectrometer to measure momentum of pion from two-body mesonic decay of electro-produced Λ hyperfragments. The aim will be to measure with high precision ground-state mass values of light Λ-hypernuclei off the stability valley. Since Λ-hypernuclei are produced from nuclear fragments, their (A, Z) combinations could spread over a large interval. Then, some hyperisotopes that are not accessible in missing-mass spectroscopy experiments, can be observed for the first time.

9.3. Strangeness physics at the Mainz Microtron

Very recently it has been realized that the Mainz Microtron (MAMI), a facility not traditionally dedicated to hypernuclear studies, could offer the opportunity to carry

out a high resolution program of decay pion spectroscopy (see subsection 2.5). The electron accelerator MAMI-C consists in fact of three stages of racetrack microtrons and one stage in the form of a double-sided harmonic microtron [252]. It is capable of delivering a continuous wave electron beam with energies ranging from 180 MeV to 1.6 GeV and currents up to 100 μA. Then, it represented a good playground to implement the same idea previously proposed to study light Λ-hypernuclei via two-body decay pion spectroscopy at JLab [253] and to perform a complementary hypernuclear physics program to the JLab one.

At MAMI-C, Λ-hypernuclei are then electro-produced via reaction $(e, e'K^+)$ on a Be target. The Kaon Spetrometer (KaoS) has been realized by integrating the preexisting A1 apparatus with a dedicated short orbit kaon spectrometer placed at $0°$ with respect to the e^- beam axis [254]. It detects kaons in the forward direction thus allowing events where strangeness production occurred to be tagged, while SpekA and SpekC, two of the three high resolution spectrometers of which the A1 apparatus is composed, allow a measurement of the momentum of pion emitted in the two-body decays of produced Λ-hyperfragments. Stopped Λ-hyperfragments are identified as monochromatic peaks in the π^- momentum spectrum, from which their ground state mass value can be finally derived with an expected precision of 50 keV/c^2.

A pilot run completed in 2011 has been followed by two data-taking campaigns in 2012 and 2014. Preliminary results of the challenging analysis performed on the first two data samples demonstrated the validity of such an approach [255–257], that has in principle the potentiality to overcome the energy resolution limitations that affected the previous measurements performed at KEK [129] and at DAΦNE [181]. Even though it is still premature to draw any final conclusion and to make any quantitative statement, the decay pion spectroscopy of electro-produced Λ-hypernuclei looks very promising. Besides providing a new set of precise hypernuclear ground states mass values, which represent an indispensable input for any structure calculation, it could address the CSB issue in $A = 4$ systems (see subsection 4.3 and subsection 9.2) thanks to a new measurement of the $^4_\Lambda$H level structure [258].

9.4. Multistrange systems study at FAIR

Some years ago the GSI management initiated a project to extend the existing facility and to offer to the scientific community an international laboratory where research with antiprotons and ions (FAIR) could be performed. The heart of the new accelerator complex is a double ring tunnel with circumference of 1100 meters, that will house 2 synchrotrons, SIS100 and SIS300. The synchrotron SIS100 will provide an intense (4×10^{13}) pulsed proton beam of 29 GeV which is suitable for an efficient $\bar{p}$ production. Details about this project can be found in [259].

$\bar{p}$s will be finally available at the High Energy Storage Ring (HESR), a slow ramping synchrotron and storage ring equipped with stochastic and electron cooling to provide excellent beam energy definition. The energy could be varied from 3.0 up to 14.5 GeV.

The antiProton ANnihilation at DArmstadt Collaboration ($\overline{P}$ANDA) is currently designing a multipurpose apparatus [260]. It will be installed on HESR to perform a large series of measurements with the aim of improving the knowledge of the strong interaction and of the hadron structure [261].

One of the main items of the physics program of this experiment is the study of the double Λ-hypernuclei. Despite the fact that the knowledge of $\Lambda\Lambda$ interaction

represents a fundamental piece of information for reaching a unified understanding of the baryon-baryon interaction in the framework of SU(3) symmetry, experimental data on this subject are very scarce. Actually besides the first, pioneering measurements of $_{\Lambda\Lambda}^{10}$Be [262] and $_{\Lambda\Lambda}^{6}$He [263], only five different nuclear species with double strangeness were recently observed and unambiguously identified, namely $_{\Lambda\Lambda}^{6}$He, $_{\Lambda\Lambda}^{10}$Be, $_{\Lambda\Lambda}^{11}$Be, $_{\Lambda\Lambda}^{12}$Be and $_{\Lambda\Lambda}^{13}$B [264]. New, high statistics data samples are then highly desirable.

As already mentioned in subsection 6.2, the most effective way to implant two units of strangeness in a nucleus is the Ξ^- atomic capture at rest. Usually Ξ^- production proceeds through the quasi-free elementary reaction $K^- + p \rightarrow \Xi^- + K^+$. An original and completely different experimental approach will be pursued at $\overline{\text{P}}$ANDA [257, 265, 266]. The basic idea is to produce a large number of $\overline{\Xi}^+ \Xi^-$ pairs through $\bar{p}$-nucleus annihilations on a primary target. The Ξ^- will be then slowed down in a secondary active target where it can form a double Λ-hypernucleus (or one or two hyperfragments). In addition the detection of $\overline{\Xi}^+$ (or of K^+ pair following its interaction in the primary target) will allow the tagging of the event.

This outlined program represents a very severe commitment since the study of double Λ-hypernuclei is neither just nor a simple extension of what has been done for the single Λ-hypernuclei. It must be noted that, since $S = -2$ hypernuclei will be produced through a two-step mechanism, it will be no longer possible to perform spectroscopic studies as in the case of $S = -1$ systems, that are generally formed in a two-body reaction. Identification and spectroscopic analysis of double Λ-hypernuclei can then only rely on the detection of their double sequential pionic decay. γ-spectroscopy could offer a possible way to partially overcome this problem, by detecting γ-rays emitted from the Ξ^- stopping target. When measured in coincidence with the known single Λ-hyperfragment γ-rays, the unknown γ-ray energies would provide information on excited levels of double Λ-hypernuclei with high precision. However, this will represent a new challenge from the instrumental point of view. In fact $\overline{\text{P}}$ANDA would be the first example of real, that is mechanical, integration of a magnetic spectrometer and a large array of HPGe detectors. To this purpose, it has been experimentally demonstrated that the crystals can be safely operated immersed in a quite strong magnetic field [267–270]. This way it will be possible to carry on a measurement complementary to the one of the ground state binding energies of double Λ-hypernuclei planned at J-PARC by the E07 Collaboration.

If successful, such a multistrange hypernuclei production method could be extended in order to produce triple Λ-hypernuclei, by exploiting the $\Omega^- \Omega^+$ pair production in $\bar{p}$ annihilation on a nuclear target.

10. Summary and outlook

Experimental hypernuclear physics is at present in a stand-by condition. Almost all the results highlighted in Sections 4–8 are actually the final analysis output of no longer running experiments like the KEK-PS series, FINUDA, JLab E01-011 and HypHI. Most of them were dedicated magnetic spectrometers installed on accelerators not, or not completely, dedicated to hypernuclear physics. More surprising is the situation for the STAR and the ALICE experiments. As discussed in Section 7, they both were designed to study heavy-ion collisions at very high energy and hypernuclei are just a single item in a wide physics program.

Many basic questions remain open in hypernuclear physics. Moreover this

research field has still a stimulating discovery potential. High-precision and high-statistics are the key requirements that must be featured by next generation experiments aiming to accept such challenges. As far as the first point is concerned, smart combination of γ-ray detector arrays and magnetic spectrometers will allow a further breakthrough in our knowledge of the details of hypernuclear energy levels. The answer to the second issue is the availability of dedicated facilities where it will be possible to collect data samples large enough to confirm with high statistical significance the experimental evidences so far reported and to study processes that we know to be characterized by very small cross section values.

In this perspective, the J-PARC commissioning and the approval of the associated hypernuclear physics program represent the main opportunity to progress in this field.

In closing this article, we list up what we think is highly desirable to see accomplished by the next decade:

- successful results from the decay pion spectroscopy program in Mainz;

- next generation γ-ray spectroscopy results by Hyperball-J detector at J-PARC;

- progress in neutron-rich Λ hypernuclear spectroscopy;

- confirmation (or confutation) of the $K^- pp$ existence from the J-PARC experiments;

- new data on Ξ and double Λ-hypernuclei from J-PARC;

- commissioning of new facilities such as FAIR and JLab 12 GeV;

- YN and YY potentials determination from lattice QCD, including the spin-dependent ones.

References

[1] ed B Juliá-Díaz *et al* 2013 *Proc. of the 11th Int. Conf. on Hypernuclear and Strange Particle Physics* 1–5 October 2012 Barcelona, Spain *Nucl. Phys.* A **914** 1–567

[2] ed B F Gibson *et al* 2010 *Proc. of the 10th Int. Conf. on Hypernuclear and Strange Particle Physics* 14–18 September 2009 Tokai, Japan *Nucl. Phys.* A **835** 1–469

[3] ed J Pochodzalla and Th Walcher 2007 *Proc. of the 9th Int. Conf. on Hypernuclear and Strange Particle Physics* 10–14 October 2006 Mainz, Germany (Berlin, Heidelberg: Società Italiana di Fisica / Springer-Verlag) 1–400

[4] Davis D H 2005 50 years of hypernuclear physics I. The early experiments *Nucl. Phys.* A **754** 3c–13c

[5] Dalitz R H 2005 50 years of hypernuclear physics II. The later years *Nucl. Phys.* A **754** 14c–24c

[6] ed A Gal and Ed Hungerford 2005 *Proc. of the 8th Int. Conf. on Hypernuclear and Strange Particle Physics* 14–18 October 2003 Newport News, VA, USA *Nucl. Phys.* A **754** 1c–489c

[7] Povh B 1987 Nuclear physics with strange particles *Prog. Part. Nucl. Phys.* **18** 183–216

[8] Chrien R E and Dover C B 1989 Nuclear systems with Strangeness *Ann. Rev. Nucl. Part. Sci.* **39** 113–50

[9] Bandō H *et al* 1990 Production, Structure, and decay of Hypernuclei *Int. J. Mod. Phys.* A **21** 4021–198

[10] Hashimoto O and Tamura H 2006 Spectroscopy of Λ hypernuclei *Prog. Part. Nucl. Phys.* **57** (2006) 564–653

[11] Botta E *et al* 2012 Strangeness nuclear physics: a critical review on selected topics *Eur. Phys. J.* A **48** 41–104

[12] ed Bydžovský P *et al* 2007 *Topics in Strangeness Nuclear Physics* Lect. Notes Phys. 724 (Berlin, Heidelberg: Springer-Verlag) 1–189

[13] ed T Bressani *et al* 2005 *Proc. of the Int. School of Physics "Enrico Fermi" - Course* **CLVIII** 22 June – 2 July, 2004 Varenna (LC), Italy (IOS Press: Amsterdam) 1–687

[14] ed M Anselmino *et al* 2008 *Proc. of the Int. School of Physics "Enrico Fermi" - Course* **CLXVII** 19 – 29 June, 2007 Varenna (LC), Italy (IOS Press: Amsterdam) 1–469

[15] Jaffe R L 1977 Perhaps a Stable Dihyperon *Phys. Rev. Lett.* **38** 195–8

[16] Tamura H *et al* 2013 Gamma-ray spectroscopy of hypernuclei – present and future *Nucl. Phys.* A **914** 99–108

[17] Millener D J 2013 Shell-model calculations applied to the γ-ray spectroscopy of light Λ hypernuclei *Nucl. Phys.* A **914** 109–18

[18] Rijken Th A *et al* 2010 Status of understanding the YN/YY-interactions Meson-exchange viewpoint *Nucl. Phys.* A **835** 160–7

[19] Rijken Th A 2006 Extended-soft-core baryon-baryon model. I. Nucleon-nucleon scattering with the ESC04 interaction *Phys. Rev.* C **73** 044007

[20] Rijken Th A and Yamamoto Y 2006 Extended-soft-core baryon-baryon model. II. Hyperon-nucleon interaction *Phys. Rev.* C **73** 044008

[21] Polinder H *et al* 2007 Strangeness S=-2 baryon-baryon interactions using chiral effective field theory *Phys. Lett.* B **653** 29–37

[22] Polinder H *et al* 2006 Hyperon-nucleon interactions–a chiral effective field theory approach *Nucl. Phys.* A **779** 244–66

[23] Haidenbauer J and Meißner U-G 2005 Jülich hyperon-nucleon model revisited *Phys. Rev.* C **72** 044005

[24] Fujiwara Y *et al* 2007 Baryon-baryon interactions in the SU_6 quark model and their applications to light nuclear systems *Prog. Part. Nucl. Phys.* **58** 439–520

[25] Valcarce A *et al* 2005 Quark-model study of few-baryon systems *Rept. Prog. Phys.* **68** 965–1042

[26] Ishii N *et al* 2007 Nuclear Force from Lattice QCD *Phys. Rev. Lett.* **99** 022001

[27] Nemura H *et al* 2009 Hyperon-nucleon force from lattice QCD *Phys. Lett.* B **673** 136–41

[28] Inoue T *et al* 2010 Baryon-Baryon Interactions in the Flavor $SU(3)$ Limit from Full QCD Simulations on the Lattice *Prog. Theor. Phys.* **124** 591–603

[29] Parreño A 2012 Binding two baryons in Lattice QCD *Nucl. Phys.* A **881** 14–27

[30] Demorest P B *et al* 2010 Shapiro Delay Measurement of A Two Solar Mass Neutron Star *Nature* **467** 1081–83

[31] Antoniadis J *et al* 2013 A Massive Pulsar in a Compact Relativistic Binary *Science* **340** 6131

[32] Danysz M and Pniewsky J 1953 Delayed Disintegration of a Heavy Nuclear Fragment: I *Phil. Mag.* **44** 348–51

[33] Feshbach H and Kerman K 1966 *Preludes in Theoretical Physics* (North Holland: Amsterdam) pp 260–78

[34] Bussa M P *et al* 2001 Light hyperfragments production in $\bar{p}$ annihilation at rest on nuclear emulsion *Nucl. Phys.* A **691** 72–5

[35] Abdurakhimov A U *et al* 1989 Experimental study of relativistic hypernuclei using the HYBS-spectrometer *Nuovo Cimento* A **102** 645–52

[36] Avramenko S *et al* 1992 A study of the production and lifetime of the lightest relativistic hypernuclei *Nucl. Phys.* A **547** 95c–100c

[37] Armstrong T A *et al* 2004 Production of $^3_\Lambda$H and $^4_\Lambda$H in central 11.5 GeV/c Au + Pt heavy ion collisions *Phys. Rev.* C **70** 024902

[38] Fukuda T *et al* 2007 The study of hypernuclei with heavy ion beams at GSI *Nucl. Phys.* A **790** 161c–66c

[39] Hungerford E V 2005 The production of hypernuclei. A strange process *Proc. of the Int. School of Physics "Enrico Fermi" - Course* **CLVIII** 22 June – 2 July, 2004 Varenna (LC), Italy ed T Bressani *et al* (IOS Press: Amsterdam) pp 55–123

[40] Bressani T 2007 Strange nuclei *Proc. of the Int. School of Physics "Enrico Fermi" - Course* **CLXVII** 19 – 29 June, 2007 Varenna (LC), Italy ed M Anselmino *et al* (IOS Press: Amsterdam) pp 3–51

[41] Garibaldi F *et al* 2013 High resolution hypernuclear spectroscopy at Jefferson Lab Hall A *Nucl. Phys.* A **914** 34–40

[42] Itonaga K *et al* 1994 Hypernuclear and Lambda spin polarizations produced in the (π^+, K^+) reaction *Phys. Rev.* C **49** 1045–58

[43] Millener D J 2001 Shell model description of Λ hypernuclei *Nucl. Phys.* A **691** 93–100

[44] Hiyama E *et al* 2000 ΛN Spin-Orbit Splittings in $^9_\Lambda$Be and $^{13}_\Lambda$C Studied with One-Boson-Exchange ΛN Interactions *Phys. Rev. Lett.* **85** 270–3

[45] Millener D J *et al* 1988 Λ-Nucleus Single Particle Potentials *Phys. Rev.* C **38** 2700–8

[46] Tanida K *et al* 2001 Measurement of the $B(E2)$ of hyper $^7_\Lambda$Li and Shrinkage of the Hypernuclear Size *Phys. Rev. Lett.* **86** 1982–85

[47] Tamura H *et al* 2000 Observation of a Spin-Flip $M1$ Transition in $^7_\Lambda$Li *Phys. Rev. Lett.* **84** 5963–6

[48] Tamura H *et al* 2001 High resolution spectroscopy of Λ hypernuclei: present status and perspectives *Nucl. Phys.* A **691** 86–92

[49] Ajimura S *et al* 2001 Observation of Spin-Orbit Splitting in Λ Single-Particle States *Phys. Rev. Lett.* **86** 4255–8

[50] Akikawa H *et al* 2002 Hypernuclear Fine Structure in $^9_\Lambda$Be *Phys. Rev. Lett.* **88** 082501

[51] Ukai M *et al* 2004 Hypernuclear Fine Structure in $^{16}_\Lambda$O and the ΛN Tensor Interaction *Phys. Rev. Lett.* **93** 232501

[52] Tamura H *et al* 2005 γ-ray spectroscopy in Λ hypernuclei *Nucl. Phys.* A **754** 58–69

[53] Tamura H *et al* 2010 Gamma spectroscopy of hypernuclei: a decade of Hyperball project and future plans at J-PARC *Nucl. Phys.* A **835** 3–10

[54] Millener D J *et al* 1985 Spin dependence of the ΛN effective interaction *Phys. Rev.* C **31** 499–509

[55] Millener D J 2007 Hypernuclear Gamma-Ray Spectroscopy and the Structure of p-shell Nuclei and Hypernuclei *Lect. Notes Phys.* **724** 31–79

[56] Gibson B F and Lehman D R 1988 Four-body calculation of the 0^+–1^+ binding energy difference in the $A = 4$ Λ hypernuclei *Phys. Rev.* C **37** 679–91

[57] Akaishi Y *et al* 2000 Coherent $\Lambda\mathcal{N}$ – $\Sigma\mathcal{N}$ Coupling in s-Shell Hypernuclei *Phys. Rev. Lett.* **84** 3539–41

[58] Pile P H *et al* 1992 A new 1-2 GeV/c separated beam for BNL *Nucl. Instrum. Methods* A **321** 48–58

[59] Fukuda T *et al* 1995 The superconducting kaon spectrometer *Nucl. Instrum. Methods* A **361** 485–96

[60] Miyoshi T *et al* 2003 High Resolution Spectroscopy of the $^{12}_\Lambda$Be Hypernucleus Produced by the $(e,e'K^+)$ Reaction *Phys. Rev. Lett.* **90** 232502

[61] Yuan L *et al* 2006 Hypernuclear spectroscopy using the $(e, e'K^+)$ reaction *Phys. Rev.* C **73** 044607

[62] Hashimoto O *et al* 2010 Hypernuclear Spectroscopy at JLab Hall C *Nucl. Phys.* A **835** 121–8

[63] Tang L *et al* 2014 Experiments with the High Resolution Kaon Spectrometer at JLab Hall C and the new spectroscopy of $^{12}_\Lambda$B hypernuclei *Phys. Rev.* C 034320

[64] Hiyama E and Yamamoto Y 2012 Structure of $^{10}_\Lambda$Be and $^{10}_\Lambda$B hypernuclei studied with the four-body cluster model *Progr. Theor. Phys.* **128** 105–24

[65] Zhang Y *et al* 2012 Structure of $^{10}_\Lambda$Be studied with the four-body cluster model *Nucl. Phys.* A **881** 288–97

[66] LeRose J J *et al* 2008 Hypernuclear spectroscopy via $(e, e'K^+)$ in JLab's Hall A *Nucl. Phys.* A **804** 116–24

[67] Cusanno F *et al* 2010 Update of High Resolution $(e, e'K^+)$ Hypernuclear Spectroscopy at Jefferson Lab's Hall A *Nucl. Phys.* A **835** 129–35

[68] De Leo R *et al* 2010 Proximity focusing RICH detector based on multilayer silica aerogel radiator *Nucl. Instrum. Methods* A **617** 381–3

[69] Brun R *et al* 1987 GEANT3 European Organization for Nuclear Research, Report No. CERN-DD-EE-84-1

[70] Feliciello A 2013 The last results from the FINUDA experiment *Mod. Phys. Lett.* A **28** 1330029

[71] Nagamiya S 2012 Introduction to J-PARC *Prog. Theor. Exp. Phys.* 02B001

[72] Ikegami M 2012 Beam commissioning and operation of the J-PARC linac *Prog. Theor. Exp. Phys.* 02B002

[73] Hotchi H *et al* 2012 Beam commissioning and operation of the Japan Proton Accelerator Research Complex 3-GeV rapid cycling synchrotron *Prog. Theor. Exp. Phys.* 02B003

[74] Koseki T *et al* 2012 Beam commissioning and operation of the J-PARC main ring synchrotron *Prog. Theor. Exp. Phys.* 02B004

[75] Sekiguchi T 2012 Neutrino facility and neutrino physics in J-PARC *Prog. Theor. Exp. Phys.* 02B005

[76] Agari K *et al* 2012 Primary proton beam line at the J-PARC hadron experimental facility *Prog. Theor. Exp. Phys.* 02B008

[77] Agari K *et al* 2012 Secondary charged beam lines at the J-PARC hadron experimental hall *Prog. Theor. Exp. Phys.* 02B009

[78] Takahashi T *et al* 2012 Beam and SKS spectrometers at the K1.8 beam line *Prog. Theor. Exp. Phys.* 02B010

[79] Agari K *et al* 2012 The K1.8BR spectrometer system at J-PARC *Prog. Theor. Exp. Phys.* 02B011

[80] Shirotori K *et al* 2012 Search for the Θ^+ Pentaquark via the $\pi^- p \to K^- X$ Reaction at 1.92 GeV/c *Phys. Rev. Lett.* **109** 132002

[81] Naruki M *et al* 2013 Search for Pentaquark Θ^+ in Hadronic Reaction at J-PARC *Few Body Syst.* **54** 955–60

[82] Moritsu M *et al* 2013 Search for the pentaquark Θ^+ at J-PARC *Nucl. Phys.* A **914** 91–6

[83] Moritsu M *et al* 2014 High-resolution search for the Θ^+ pentaquark via a pion-induced reaction at J-PARC *Phys. Rev.* C **90** 035205

[84] Ichikawa Y *et al* 2013 J-PARC E27 Experiment to Search for a Nuclear Kaon Bound State $K^- pp$ *Few Body Syst.* **54** 1191–4

[85] Ichikawa Y *et al* 2014 Inclusive spectrum of the $d(\pi^+, K^+)$ reaction at 1.69 GeV/c *Prog. Theor. and Exp. Phys.* 101D03

[86] Agnello M *et al* 2005 First results on $^{12}_{\Lambda}$C production at DAΦNE *Phys. Lett.* B **622** 35–44

[87] Iodice M *et al* 2007 High Resolution Spectroscopy of $^{12}_{\Lambda}$B by Electroproduction *Phys. Rev. Lett.* **99** 052501

[88] Itonaga K *et al* 1990 p-Shell Hypernuclei via (K^-,π^-), (π^+,K^+) and (Stopped K^-,π^-) Reactions *Prog. Theor. Phys.* **84** 291–316

[89] Hasegawa T *et al* 1995 Core-Excited States of $^{12}_{\Lambda}$C Hypernuclei Formed in the (π^+,K^+) reaction *Phys. Rev. Lett.* **74** 224-7

[90] Gal A 1995 Hypernuclei: a theoretical review *Physics and Detectors for DAΦNE* (Frascati Physics Series **IV**) April 4–7, 1995 Frascati (RM), Italy ed R Baldini *et al* (SIS-LNF: Frascati (RM)) pp 315–331

[91] Agnello M *et al* 2011 Hypernuclear spectroscopy with K^- at rest on ^{7}Li, ^{9}Be, ^{13}C and ^{16}O *Phys. Lett.* B **698** 219–25

[92] Tamura H *et al* 1989 Study of Λ Hypernuclei with Stopped K^- Reactions *Progr. Theor. Phys. Suppl.* **117** 1–15

[93] Cusanno F *et al* 2009 High Resolution Spectroscopy of $^{12}_{\Lambda}$N by Electroproduction *Phys. Rev. Lett.* **103** 202501

[94] Cieplý A *et al* 2011 Constraints on the threshold K^- nuclear potential from FINUDA (K^-_{stop}, π^-) hypernuclear spectra *Phys. Lett.* B **698** 226–30

[95] Ma Y *et al* 2007 γ-ray spectroscopy study of $^{11}_{\Lambda}$B and $^{12}_{\Lambda}$C *Eur. Phys. J.* A **33** 243–6

[96] Ma Y *et al* 2010 Updated results on the $^{11}_{\Lambda}$B and $^{12}_{\Lambda}$C γ-ray spectroscopy study *Nucl. Phys.* A **835** 422–5

[97] Hosomi K *et al* Gamma-ray spectroscopy of $^{12}_{\Lambda}$C via the (π^+, K^+) reaction 2013 *Nucl. Phys.* A **914** 184-8

[98] Takahashi T *et al* 2000 Spectroscopy of light Λ hypernuclei *Nucl. Phys.* A **670** 265–8

[99] Hotchi H *et al* 2001 Spectroscopy of medium heavy lambda hypernuclei via the (π^+, K^+) reaction *Phys. Rev.* C **64** 044302

[100] Millener D J 2008 Shell-model interpretation of γ-ray transitions in p-shell hypernuclei *Nucl. Phys.* A **804** 84–98

[101] Ukai M *et al* 2008 γ-ray spectroscopy of $^{16}_{\Lambda}$O and $^{15}_{\Lambda}$N hypernuclei via ^{16}O$(K^-, \pi^- \gamma)$ reaction *Phys. Rev.* C **77** 054315

[102] Millener D J 2010 Shell-model structure of light hypernuclei *Nucl. Phys.* A **835** 11–8

[103] Dalitz R H and Levi Setti R 1963 Some possibilities for unusual light hypernuclei *Nuovo Cimento* **30** 489–501

[104] Schaffner-Bielich J 2008 Hypernuclear Physics for Neutron Stars *Nucl. Phys.* A **804** 309–21

[105] Schaffner-Bielich J 2010 Strangeness in Compact Stars *Nucl. Phys.* A **835** 279–86

[106] Vidaňa I *et al* 2011 Estimation of the effect of hyperonic three-body forces on the maximum mass of neutron stars *Europhys. Lett.* **94** 11002

[107] Klähn T *et al* 2013 Implications of the measurement of pulsars with two solar masses for quark matter in compact stars and heavy-ion collisions: A NambuJona-Lasinio model case study *Phys. Rev.* D **88** 085001

[108] Lattimer J M and Steiner A W 2014 Neutron Star Masses and Radii from Quiescent Low-Mass X-ray Binaries *The Astrophysical Journal* **784** 123

[109] Umeya A and Harada T 2009 Λ-Σ coupling effect in the neutron-rich Λ hypernucleus $^{10}_{\Lambda}$Li in a microscopic shell-model calculation *Phys. Rev.* C **79** 024315

[110] Harada T 2010 Neutron-rich Hypernuclei *Nucl. Phys.* A **835** 136-43

[111] Umeya A and Harada T 2010 Shell-model study of Σ-mixing in neutron-rich $_{\Lambda}$Li hypernuclei *Nucl. Phys.* A **835** 426-9

[112] Umeya A and Harada T 2010 Σ-admixture in neutron-rich Li Λ hypernuclei in a microscopic shell-model calculation *EPJ Web Conf.* **3** 07012

[113] Umeya A and Harada T 2011 Doublet-spacing enhancement caused by ΛN-ΣN coupling in $_{\Lambda}$Li hypernuclear isotopes *Phys. Rev.* C **83** 034310

[114] Akaishi Y and Yamazaki T 1999 Strangeness in nuclear matter *Physics and Detectors for DAΦNE* (Frascati Physics Series **XVI**) November 16–19, 1999 Frascati (RM), Italy ed S Bianco *et al* (SIS-LNF: Frascati (RM)) pp 59–74

[115] Myint K S *et al* 2000 Neutron rich Λ hypernuclei *Few Body Syst. Suppl.* **12** 383–86
[116] Myint K S and Akaishi Y 2002 Coherent Λ-Σ Coupling and ΛNN Three-Body Force in Neutron-Excess Nuclei *Progr. Theor. Phys. Suppl.* **146** 599–600
[117] Shinmura S *et al* 2002 Coherent Λ-Σ^0 mixing in high-density neutron matter *J. Phys. G* **28** L1–7
[118] Akaishi Y and Myint K S 2007 ΛNN Three-Body Force due to Coherent Λ-Σ Coupling *New Facet of Three Nucleon Force - 50 Years of Fujita Miyazawa Three Nucleon Force* AIP Conf. Proc. **1011** October 29–31, 2007, Tokyo, Japan ed H Sakai *et al* (AIP Publishing: Melville) pp 277–86
[119] Akaishi Y 2010 ΛNN Three-Body Force Due to Coherent Λ-Σ Coupling *Prog. Theor. Phys. Suppl.* **186** 378–83
[120] Majling L 1995 Production of Λ-hypernuclei with a large neutron excess and a neutron halo *Nucl. Phys. A* **585** 211c–14c
[121] Jurić M *et al* 1973 A new determination of the binding-energy values of the light hypernuclei (A ⩽ 15) *Nucl. Phys. B* **52** 1–30
[122] Tilley D R *et al* 2004 Energy levels of light nuclei A = 8, 9, 10 *Nucl. Phys. A* **745** 155–362
[123] Chrien R E *et al* 1992 Two nucleon production of hyperons and the search for strange dibaryons *Czech. J. Phys.* **42** 1089–113
[124] Kubota K *et al* 1996 Search for neutron-rich Λ hypernuclei in the $(K^-_{\text{stopped}}, \pi^+)$ reaction *Nucl. Phys. A* **602** 327–33
[125] Saha P K *et al* 2005 Production of the Neutron-Rich Hypernucleus $^{10}_{\Lambda}$Li in the (π^-, K^+) Double Charge-Exchange Reaction *Phys. Rev. Lett.* **94** 052502
[126] Agnello M *et al* 2006 Search for $^6_{\Lambda}$H and $^7_{\Lambda}$H with the $(K^-_{\text{stop}}, \pi^+)$ reaction *Phys. Lett. B* **640** 145–49
[127] Agnello M *et al* 2012 Evidence for Heavy Hyperhydrogen $^6_{\Lambda}$H *Phys. Rev. Lett.* **108** 042501
[128] Agnello M *et al* 2012 First observation of the hyper superheavy hydrogen $^6_{\Lambda}$H *Nucl. Phys. A* **881** 269–87
[129] Tamura H *et al* 1989 Formation of $^4_{\Lambda}$H Hyperfragment From K^- Absorption at Rest on Light Nuclei *Phys. Rev. C* **40** 479–82
[130] Hiyama E *et al* 2013 Four-body structure of neutron-rich hypernucleus $^6_{\Lambda}$H *Nucl. Phys. A* **908** 29–39
[131] Gal A and Millener D J 2013 Neutron-rich hypernuclei: $^6_{\Lambda}$H and beyond *Phys. Lett. B* **725** 445–50
[132] Sugimura H *et al* 2014 Search for $^6_{\Lambda}$H hypernucleus by the ^{6}Li(π^-, K^+) reaction at $p_{\pi^-} = 1.2$ GeV/c *Phys. Lett. B* **729** 39–44
[133] Agnello M *et al* 2012 Search for neutron-rich hypernucleus $^9_{\Lambda}$He *Phys. Rev. C* **86** 057301
[134] Nakamura S N *et al* 2013 Observation of the $^7_{\Lambda}$He Hypernucleus by the $(e, e'K^+)$ Reaction *Phys. Rev. Lett.* **110** 012502
[135] Hiyama E *et al* 2009 Structure of A=7 iso-triplet Λ hypernuclei studied with the four-body cluster model *Phys. Rev. C* **80** 054321
[136] Nogga A *et al* 2002 The hypernuclei $^4_{\Lambda}$He and $^4_{\Lambda}$H: Challenges for Modern Hyperon-Nucleon Forces *Phys. Rev. Lett.* **88** 172501
[137] Gibson B F *et al* 1972 Effects of Λ-Σ Coupling in $^4_{\Lambda}$H, $^4_{\Lambda}$He, and $^5_{\Lambda}$He *Phys. Rev. C* **6** 741–8
[138] Bodmer A R and Usmani Q N 1985 Coulomb effects and charge symmetry breaking for the $A = 4$ hypernuclei *Phys. Rev. C* **31** 1400–11
[139] Cheston W and Primakoff H 1953 "Nonmesonic" Bound V-Particle Decay *Phys. Rev.* **92** 1537–41
[140] Alberico W M and Garbarino G 2002 Weak decay of Lambda hypernuclei *Phys. Rep.* **369** 1–109
[141] Alberico W M and Garbarino G 2005 Weak decay of hypernuclei *Proc. of the Int. School of Physics "Enrico Fermi" - Course* **CLVIII** 22 June – 2 July, 2004 Varenna (LC), Italy ed T Bressani *et al* (IOS Press: Amsterdam) pp 125–81
[142] Outa H 2005 Experiments on hypernuclear weak decays *Proc. of the Int. School of Physics "Enrico Fermi" - Course* **CLVIII** 22 June – 2 July, 2004 Varenna (LC), Italy ed T Bressani *et al* (IOS Press: Amsterdam) pp 219–58
[143] Szymanski J J *et al* 1991 Nonleptonic weak decay of $^5_{\Lambda}$He and $^{12}_{\Lambda}$C *Phys. Rev. C* **43** 849–62
[144] Noumi H *et al* 1995 Hypernuclear weak decay of $^{12}_{\Lambda}$C and $^{11}_{\Lambda}$B *Phys. Rev. C* **52** 2936–45
[145] Noumi H *et al* 1995 Measurement of $^5_{\Lambda}$He weak decay branching ratios *Proc. of the IV Int. Symp. on Weak and Electromagnetic Interaction in Nuclei* Osaka, Japan, June 12-16, 1995 ed H R Jiri *et al* (World Scientific: River Edge) pp 550–3
[146] Alberico W M *et al* 1991 Two-nucleon induced Λ decay in nuclei *Phys. Lett. B* **256** 134–40

[147] Bauer E and Garbarino G 2009 Exchange terms in the two-nucleon induced non-mesonic weak decay of Λ-hypernuclei *Nucl. Phys.* A **828** 29–51

[148] Cohen J 1990 Weak Non-mesonic Decays of Λ Hypernuclei *Progr. Part. Nucl. Phys.* **25** 139–234

[149] Parreño A 2007 Weak decays of hypernuclei *Lect. Notes. Phys.* **724** 141–89

[150] Prem R J and Steinberg P H 1964 Lifetimes of Hypernuclei, $_\Lambda H^3$, $_\Lambda H^4$, $_\Lambda He^5$ *Phys. Rev.* **136** B1803

[151] Kang Y W *et al* 1965 Lifetimes of Light Hyperfragments *Phys. Rev.* **139** B401

[152] Phillips R E *et al* 1969 Lifetimes of Light Hyperfragments. II *Phys. Rev.* **180** 1307–18

[153] Bohm G *et al* 1970 On the lifetime of the $_\Lambda^3 H$ hypernucleus *Nucl. Phys.* B **16** 46–52

[154] Bohm G *et al* 1970 A measurement of the lifetime of the $_\Lambda^5 He$ hypernucleus *Nucl. Phys.* B **23** 93–8

[155] Keyes G *et al* 1968 New Measurement of the $_\Lambda H^3$ Lifetime *Phys. Rev. Lett.* **20** 819–21

[156] Keyes G *et al* 1970 Properties of $_\Lambda H^3$ *Phys. Rev.* D **1** 66–77

[157] Keyes G *et al* 1973 A measurement of the lifetime of the $_\Lambda^3 H$ hypernucleus *Nucl. Phys.* B **67** 269–83

[158] Grace R *et al* 1985 Weak Decay of $_\Lambda^{12} C$ and $_\Lambda^{11} B$ Hypernuclei *Phys. Rev. Lett.* **55** 1055

[159] Outa H *et al* 1995 Mesonic weak decay of $_\Lambda^4 H$ and $_\Lambda^4 He$ *Nucl. Phys.* A **585** 109c–12c

[160] Outa H *et al* 1998 Mesonic and non-mesonic decay widths of $_\Lambda^4 H$ and $_\Lambda^4 He$ *Nucl. Phys.* A **639** 251c–60c

[161] Zeps V J *et al* 1998 The weak decays of light hypernuclei *Nucl. Phys.* A **639** 261c–8c

[162] Park H *et al* 2000 Lifetime measurements of medium-heavy Λ hypernuclei *Phys. Rev.* C **61** 054004

[163] Kameoka S *et al* 2005 Measurement of the π^- decay width of $_\Lambda^5 He$ *Nucl. Phys.* A **754** 173c–7c

[164] Parker J D *et al* 2007 Weak decays of $_\Lambda^4 He$ *Phys. Rev.* C **76** 035501

[165] Nield K J *et al* 1976 Production of hypernuclei in a 2.1 GeV/nucleon oxygen beam *Phys. Rev.* C **13** 1263–6

[166] Noga V I *et al* 1986 Delayed Fission Of Products From Interaction Of Electrons With An Energy Of 1200-mev With Bismuth Nuclei *Sov. J. Nucl. Phys.* **43** 856

[167] Bocquet J P *et al* 1987 Delayed fission from the antiproton annihilation in ^{209}Bi – evidence for hypernuclear decay *Phys. Lett.* B **192** 312–4

[168] Armstrong T A *et al* 1993 Fission of heavy hypernuclei formed in antiproton annihilation *Phys. Rev.* C **47** 1957–69

[169] Cassing W *et al* 2003 Lifetime of heavy hypernuclei and its implications on the weak ΛN interaction *Eur. Phys. J.* A **16** 549–61

[170] Abelev B I *et al* 2010 Observation of an Antimatter Hypernucleus *Science* **328** 58–62

[171] Zhu Y *et al* 2013 Beam Energy Scan on Hypertriton Production and Lifetime Measurement at RHIC STAR *Nucl. Phys.* A **904–905** 551c–4c

[172] Rappold C *et al* 2013 Hypernuclear spectroscopy of products from ^6Li projectiles on a carbon target at 2 A GeV *Nucl. Phys.* A **913** 170–84

[173] Dalitz R H 1963 The hypernucleus $_\Lambda Li^8$ and the decay process $_\Lambda Li^8 \rightarrow \pi^- + {}^4He + {}^4He$ *Nucl. Phys.* **41** 78–91

[174] Ziemińska D 1975 The decay process $_\Lambda B^{11} \rightarrow \pi^- + {}^{11}C$ *Nucl. Phys.* A **242** 461–6

[175] Ziemińska D and Dalitz R H 1975 The hypernucleus $_\Lambda^{12} B$ and the decay process $_\Lambda^{12} B \rightarrow \pi^- + 3\alpha$ *Nucl. Phys.* A **238** 453–90

[176] Kiełczewska D *et al* 1980 A determination of the spin of the hypernucleus $_\Lambda^{12} B$:(II). A complete analysis *Nucl. Phys.* A **333** 367–80

[177] Bertrand D *et al* 1970 Branching ratios for the π^- mesonic decays of the hypernuclei $_\Lambda^3 H$ and $_\Lambda^4 H$ *Nucl. Phys.* B **16** 77–84

[178] Bloch M M *et al* 1964 Hyperfragment studies in the Helium bubble chamber *Proc. of Int. Conf. on Hyperfragments* 28 – 30 March, 1963 St. Cergue, Switzerland ed W O Lock (CERN64-1) pp 63–74

[179] Davis D H *et al* 1963 A determination of the spin of $_\Lambda Li^8$ *Nucl. Phys.* **41** 73–7

[180] Okada S *et al* 2005 π^0 decay branching ratios of $_\Lambda^5 He$ and $_\Lambda^{12} C$ hypernuclei *Nucl. Phys.* A **754** 178c–83c

[181] Agnello M *et al* and Gal A 2009 New results on mesonic weak decay of p-shell Λ-hypernuclei *Phys. Lett.* B **681** 139–46

[182] Motoba T *et al* 1991 Continuum pion spectra in the weak decays of $_\Lambda^4 H$, $_\Lambda^5 He$ and $_{\Lambda\Lambda}^6 He$ *Nucl. Phys.* A **534** 597–619

[183] Bandō H *et al* 1992 Strangeness nuclear physics *Perspectives of Meson Science* ed T Yamazaki *et al* (North Holland: Amsterdam) pp 571–660

[184] Motoba T *et al* 1988 π Mesonic Decay of Light Λ Hypernuclei *Nucl. Phys.* A **489** 683–715

[185] Motoba T and Itonaga K 1994 Pi-Mesonic Weak Decay Rates of Light-to-Heavy Hypernuclei *Progr. Theor. Phys. Suppl.* **117** 477–98

[186] Sato Y *et al* 2005 Mesonic and nonmesonic weak decay widths of medium-heavy Λ hypernuclei *Phys. Rev.* C **71** 025203

[187] Sasao J *et al* 2004 $^7_\Lambda$Li ground-state spin determined by the yield of γ-rays subsequent to weak decay *Phys. Lett.* B **579** 258–64

[188] Montwill A *et al* 1974 The non-mesonic to π^- mesonic decay ratio and Λ-neutron stimulation fraction for p-shell hypernuclei *Nucl. Phys.* A **234** 413–28

[189] Gal A 2009 π^- decay rates of *p*-shell hypernuclei revisited *Nucl. Phys.* A **828** 72–83

[190] Agnello M *et al* 2012 Hypernuclear weak decay studies with FINUDA *Nucl. Phys.* A **881** 322–38

[191] Garbarino G *et al* 2004 Towards a solution of the Γ_n/Γ_p puzzle in the nonmesonic weak decay of Λ hypernuclei *Phys. Rev.* C **69** 054603

[192] Okada S *et al* 2004 Neutron and proton energy spectra from the non-mesonic weak decays of $^5_\Lambda$He and $^{12}_\Lambda$C *Phys. Lett.* B **579** 249–56

[193] Kim M *et al* 2009 Three-Body Nonmesonic Weak Decay of the $^{12}_\Lambda$C Hypernucleus *Phys. Rev. Lett.* **103** 182502

[194] Agnello M *et al* 2008 Measurement of the proton spectra from non-mesonic weak decay of $^5_\Lambda He$, $^7_\Lambda Li$ and $^{12}_\Lambda C$ *Nucl. Phys.* A **804** 151–61

[195] Agnello M *et al* and Garbarino G 2010 Proton spectra from Non-Mesonic Weak Decay of p-shell Λ-Hypernuclei and evidence for the two-nucleon induced process *Phys. Lett.* B **685** 247–52

[196] Bauer E *et al* 2010 Single and double coincidence nucleon spectra in the weak decay of Λ-hypernuclei *Nucl. Phys.* A **836** 199–224

[197] Bhang H *et al* 2007 The quenching of nucleon yields in the nonmesonic weak decay of Λ-hypernuclei and the three-body weak decay process *Eur. Phys. J.* A **33** 259–63

[198] Agnello M *et al* and Garbarino G 2011 Neutron-proton coincidences from Non Mesonic Weak Decay of p-shell Λ-hypernuclei and determination of the two-nucleon induced process *Phys. Lett.* B **701** 556–61

[199] Bauer E and Garbarino G 2010 Role of ground-state correlations in hypernuclear nonmesonic weak decay *Phys. Rev.* C **81** 064315

[200] Batty C J 1979 Nuclear bound states of negatively charged hadrons? *Phys. Lett.* B **87** 324–26

[201] Batty C J *et al* 1983 Are narrow Σ hypernuclear states consistent with σ^- atomic data? *Nucl. Phys.* A **402** 349–65

[202] Bertini R *et al* 1980 Hypernuclei with sigma particles *Phys. Lett.* B **90** 375–78

[203] Dover C B *et al* 1989 On the production and spectroscopy of Σ hypernuclei *Phys. Rep.* **184** 1–97

[204] Sawafta R *et al* 1995 Do narrow Σ hypernuclear states exist? *Nucl. Phys.* A **585** 103c–8c

[205] Bart S *et al* 1999 Σ Hyperons in the Nucleus *Phys. Rev. Lett.* **83** 5238–41

[206] Powers R J *et al* 1993 Strong-interaction effect measurements in sigma hyperonic atoms of W and Pb *Phys. Rev.* C **47** 1263–73

[207] Batty C J *et al* 1994 Density dependence of the Σ nucleus optical potential derived from Σ^- atom data *Phys. Lett.* B **335** 273–8

[208] Batty C J *et al* 1994 Density Dependence in Σ^- Atoms and Implications for Σ Hypernuclei *Prog. Theor. Phys. Suppl.* **117** 227–40

[209] Mareš J *et al* 1995 Constraints on Σ-nucleus dynamics from dirac phenomenology of Σ^- atoms *Nucl. Phys.* A **594** 311–24

[210] Hayano R S *et al* 1989 Evidence for a bound state of the $^4_\Sigma$He hypernucleus *Phys. Lett.* B **231** 355–8

[211] Outa H *et al* 1994 Formation and Decay of Σ Hypernuclei in (Stopped $K^-, \pi^\pm$) Reactions *Prog. Theor. Phys. Suppl.* **117** 177–99

[212] Nagae T *et al* 1998 Observation of a $^4_\Sigma$He Bound State in the ^{4}He(K^-, π^-) Reaction at 600 MeV/c *Phys. Rev. Lett.* **80** 1605-9

[213] Harada T *et al* 1990 Structure of the $^4_\Sigma$He hypernuclear bound state *Nucl. Phys.* A **507** 715–30

[214] Harada T 1998 *Phys. Rev. Lett.* Calculation of the $^4_\Sigma$He Bound State in the ^{4}He(K^-, π^-) Reaction at 600 MeV/c **81** 5287–90

[215] Noumi H *et al* 2002 Sigma-Nucleus Potential in $A = 28$ *Phys. Rev. Lett.* **89** 072301

[216] Noumi H *et al* 2003 Sigma-Nucleus Potential in $A = 28$ *Phys. Rev. Lett.* **90** 049902

[217] Saha P K *et al* 2004 Σ-nucleus potential studied with the (π^-, K^+) reaction on medium-to-heavy nuclear targets *Phys. Rev.* C **70** 044613

[218] Harada T and Hirabayashi Y 2005 Is the Σ-nucleus potential for Σ^- atoms consistent with the ^{28}Si(π^-, K^+) data? *Nucl. Phys.* A **759** 143–69

[219] Takahashi H *et al* 2001 Observation of a $_{\Lambda\Lambda}^{6}$He Double Hypernucleus *Phys. Rev. Lett.* **87** 212502
[220] Khaustov P *et al* 2000 Evidence of Ξ hypernuclear production in the ^{12}C$(K^-, K^+)_{\Xi}^{12}$Be reaction *Phys. Rev. C* **61** 054603
[221] Dover C B *et al* 1994 On the production and decay of strangeness S = -2 hypernuclei *Nucl. Phys. A* **572** 85–111
[222] Dover C B and Gal A 1983 Ξ Hypernuclei *Ann. of Phys.* **146** 309–48
[223] Fukuda T *et al* 1998 Search for $\Lambda\Lambda$ hypernuclei by sequential pionic decays *Nucl. Phys. A* **639** 355c–61c
[224] Yamamoto Y *et al* 1992 Formation of Double-Λ Hypernucleus from Quasi-Free Ξ^- Absorption *Progr. Theor. Phys.* **88** 1163–72
[225] Ahn J K *et al* 2001 Production of $_{\Lambda\Lambda}^{4}$H Hypernuclei *Phys. Rev. Lett.* **87** 132504
[226] Aoki S *et al* 1991 Direct observation of sequential weak decay of a double hypernucleus *Progr. Theor. Phys.* **85** 1287–98
[227] Ahn J K *et al* 2013 Double-Λ hypernuclei observed in a hybrid emulsion experiment *Phys. Rev. C* **88** 014003
[228] Ahn J K *et al* 2006 Measurement of the $\Sigma^- p$ scattering cross sections at low energy *Phys. Lett. B* **633** 214–18
[229] Tamagawa T *et al* 2001 The ΞN interaction in quasi-free Ξ^- production *Nucl. Phys. A* **691** 234–37
[230] Fukuda T *et al* 1998 Cascade hypernuclei in the (K^-, K^+) reaction on ^{12}C *Phys. Rev. C* **58** 1306–9
[231] Chen J H *et al* 2009 Observation of hypertritons in Au+Au collisions at $\sqrt{s_{NN}} = 200$ GeV *Nucl. Phys. A* **830** 761c–4c
[232] Chen J H *et al* 2010 Hypernucleus physics at RHIC *Nucl. Phys. A* **835** 117–20
[233] Lea R *et al* 2013 Hypernuclear production in Pb-Pb collision at $\sqrt{s_{NN}} = 2.76$ TeV with ALICE at the LHC *Nucl. Phys. A* **914** 415–20
[234] Bazzi M *et al* 2011 A new measurement of kaonic hydrogen X-rays *Phys. Lett. B* **704** 113–17
[235] Bazzi M *et al* 2012 Kaonic hydrogen X-ray measurement in SIDDHARTA *Nucl. Phys. A* **881** 88–97
[236] Ikeda Y *et al* 2012 Chiral SU(3) theory of antikaon-nucleon interactions with improved threshold constraints *Nucl. Phys. A* **881** 98–114
[237] Hyodo T 2013 Recent developments in antikaon-nucleon dynamics *Nucl. Phys. A* **914** 260–9
[238] Gal A 2013 Recent studies of kaonic atoms and nuclear clusters *Nucl. Phys. A* **914** 270–9
[239] Nagae T 2012 Experimental searches for antikaonic clusters *Nucl. Phys. A* **881** 141–9
[240] Agnello M *et al* 2005 Evidence for a Kaon-Bound State $K^- pp$ Produced in K^- Absorption Reactions at Rest *Phys. Rev. Lett.* **94** 212303
[241] Magas V K *et al* 2006 Critical view on the deeply bound $K^- pp$ system *Phys. Rev. C* **74** 025206
[242] Sato M *et al* 2008 Search for strange tribaryon states in the inclusive ^{4}He$(K^-_{\text{stopped}}, p)$ reaction *Phys. Lett. B* **659** 107–12
[243] Yim H *et al* 2010 Search for strange tribaryons in the ^{4}He$(K^-_{\text{stop}}, n\pi^\pm)$ reaction *Phys. Lett. B* **688** 43–9
[244] Bendiscioli G *et al* 2009 A new analysis improving the evidence of a narrow peak in the invariant-mass distribution of the Λp system observed in the $\bar{p}$ annihilation at rest on ^{4}He *Eur. Phys. J. A* **40** 11–22
[245] Bendiscioli G *et al* 2007 Search for signals of bound $\overline{K}$ nuclear states in antiproton-^{4}He annihilations at rest *Nucl. Phys. A* **789** 222–42
[246] Yamazaki T *et al* 2010 Indication of a Deeply Bound and Compact $K^- pp$ State Formed in the $pp \to p\Lambda K^+$ Reaction at 2.85 GeV *Phys. Rev. Lett.* **104** 132502
[247] Kienle P *et al* 2012 Formation of the S = -1 resonance X(2265) in the reaction $pp \to X + K^+$ at 2.50 and 2.85 GeV *Eur. Phys. J. A* **48** 183
[248] Kishimoto T *et al* 2007 Kaon-Nucleus Interaction Studied through the In-Flight (K^-, N) Reaction *Prog. Theor. Phys.* **118** 181–6
[249] Tokiyasu A O *et al* 2014 Search for the $K^- pp$ bound state via $\gamma d \to K^+ \pi^- X$ reaction at E$_\gamma$ = 1.5–2.4 GeV *Phys. Lett. B* **728** 616–21
[250] Ichikawa Y *et al* 2015 Observation of the "$K^- pp$"-like structure in the $d(\pi^+, K^+)$ reaction at 1.69 GeV/c *Prog. Theor. Exp. Phys.* 021D01
[251] Yamazaki T and Akaishi Y 2007 Basic $\overline{K}$ nuclear cluster, $K^- pp$, and its enhanced formation in the $p + p \to K^+ + X$ reaction *Phys. Rev. C* **76** 045201
[252] Kaiser K-H *et al* 2008 The 1.5-GeV harmonic double-sided microtron at Mainz University *Nucl. Instrum. Methods A* **593** 159–70
[253] Tang L 2010 New era: study light hypernuclei via two body decay pion spectroscopy using

CEBAF beam *Int. J. Mod. Phys* E **19** 2638–43
[254] Achenbach P *et al* 2011 Strange hadrons – strangeness in strongly interacting particles *Eur. Phys. J.* ST **198** 307–27
[255] Tsukada K *et al* 2013 Decay Pion Spectroscopy of Electro-Produced Hypernuclei *Few Body Syst.* **54** 375–9
[256] Achenbach P *et al* 2013 Recent Studies of Hypernuclei Formation with Electron Beams at MAMI *Few Body Syst.* **55** 887–92
[257] Esser A *et al* 2013 Prospect for hypernuclear physics at Mainz: from KAOS@MAMI to PANDA@FAIR *Nucl. Phys.* A **914** 519–29
[258] Nakamura S N *et al* 2013 Study of hypernuclei with electron beams *Nucl. Phys.* A **914** 3–13
[259] Lehrach A 2011 Performance and perspectives of hadron storage rings PoS STORI11 (2011) 066 1–9
[260] Kotulla M *et al* 2005 $\overline{\text{P}}$ANDA: Strong Interaction Studies with Antiprotons FAIR-ESAC/Pbar/Technical Progress Report 1–383
[261] Erni W *et al* 2009 Physics Performance Report for $\overline{\text{P}}$ANDA: Strong Interaction Studies with Antiprotons hep-ex/0903.3905 1–204
[262] Danysz M *et al* 1963 The identification of a double hyperfragment *Nucl. Phys.* **49** 121–32
[263] Prowse D J 1966 $_{\Lambda\Lambda}^{6}$He double hyperfragment *Phys. Rev. Lett.* **17** 782–5
[264] Nakazawa K *et al* 2010 Double-Lambda Hypernuclei Via The Ξ^- Hyperon Capture At Rest Reaction In a Hybrid Emulsion *Nucl. Phys.* A **835** 207–14
[265] Pochodzalla J 2004 Future experiments on hypernuclei and hyperatoms *Nucl. Instrum. Methods* B **214** 149–52
[266] Feliciello A *et al* 2007 Hypernuclear studies at FAIR with $\overline{\text{P}}$ANDA *Nucl. Phys.* A **790** 651c–4c
[267] Sanchez Lorente A *et al* 2007 Performance of HPGe detectors in high magnetic fields *Nucl. Instrum. Methods* A **573** 410–7
[268] Szymańska K *et al* 2008 Resolution, efficiency and stability of HPGe detector operating in a magnetic field at various gamma-ray energies *Nucl. Instrum. Methods* A **592** (2008) 486–92
[269] Agnello M *et al* 2009 Study of the performance of HPGe detectors operating in very high magnetic fields *Nucl. Instrum. Methods* A **606** 560–8
[270] Bressani T and Feliciello A 2010 HPGe In Magnetic Fields *Nucl. Phys. News.* **20** (02) 23–6